Nature-Based Secondary Resource Recovery under Climate Change Uncertainty: A Robust Multi-Objective Optimisation Methodology

Khaled Alshehri, Mohadese Basirati, Devin Sapsford, Michael Harbottle, Peter Cleall

sustainability

MDPI

Article

Nature-Based Secondary Resource Recovery under Climate Change Uncertainty: A Robust Multi-Objective Optimisation Methodology

Khaled Alshehri [1,2,*], Mohadese Basirati [3], Devin Sapsford [1], Michael Harbottle [1] and Peter Cleall [1]

[1] School of Engineering, Cardiff University, Cardiff CF24 3AA, UK; sapsforddj@cardiff.ac.uk (D.S.); cleall@cardiff.ac.uk (P.C.)
[2] Department of Civil Engineering, College of Engineering, University of Bisha, P.O. Box 001, Bisha 61922, Saudi Arabia
[3] Mines Saint-Etienne, Université Clermont Auvergne, INP Clermont Auvergne, CNRS, UMR 6158 LIMOS, 42023 Saint-Etienne, France; mohadese.basirati@emse.fr
* Correspondence: alshehrikm@cardiff.ac.uk or kalshehri@ub.edu.sa

Abstract: The management of high-volume (HV) waste poses a persistent challenge in sustainable materials management and represents an untapped opportunity in circular economy models. This study proposes a conceptual decision-making framework to operationalise a novel circular economy strategy for HV waste, involving temporary storage to facilitate nature-based secondary resource recovery. Using an illustrative case study of a candidate HV waste (legacy mining waste), we apply a robust multi-objective spatial optimisation approach at a national scale, employing an exact solution approach. Our methodology integrates mixed-integer linear programming to evaluate the economic viability, social benefits, and impacts of climate change uncertainties on nature-based solutions (NbS) implementation across diverse scenarios. The results demonstrate that NbS can enhance economic feasibility by incorporating carbon sequestration and employment benefits while demonstrating resilience against climate change projections to ensure long-term sustainability. The findings suggest that although NbS can improve the circular economy of HV nationally, it is essential to assess additional ecosystem services and address multiple uncertainties for effective macro-level sustainability assessment of HV management. This study offers a robust decision-making framework for policymakers and stakeholders to plan and implement nature-based circular economy strategies for HV waste streams at a national level while effectively managing long-term planning uncertainties.

Keywords: nature-based solutions; circular economy; resource recovery; climate change resilience; robust optimisation; multi-objective optimisation

Citation: Alshehri, K.; Basirati, M.; Sapsford, D.; Harbottle, M.; Cleall, P. Nature-Based Secondary Resource Recovery under Climate Change Uncertainty: A Robust Multi-Objective Optimisation Methodology. *Sustainability* **2024**, *16*, 7220. https://doi.org/10.3390/su16167220

Academic Editor: Md. Mizanur Rahman

Received: 8 July 2024
Revised: 13 August 2024
Accepted: 15 August 2024
Published: 22 August 2024

1. Introduction

Sustainable management of high-volume (HV) waste streams remains a significant challenge within the confines of a linear economy [1], characterised by a 'take, make, dispose' approach resulting in inefficient resource use and increased environmental degradation [2]. The concept of a circular economy (CE) has gained significant traction as a sustainable alternative to the traditional linear economy [3] where resources are continuously cycled back into the production system, minimising waste and reducing the need for virgin materials [4,5]. Nature-based solutions (NbS), which engineer natural processes to address environmental challenges, have emerged as a powerful enabler of the circular economy, particularly for the recovery of secondary resource materials [6]. NbS leverage natural processes and ecosystems to address societal challenges, including waste management and resource recovery [1]. By engineering natural processes, it is possible to reclaim valuable materials from waste streams, thereby contributing to resource efficiency and sustainability [7].

However, several HV waste flows remain underutilised (e.g., combustion ash, dredging, alkaline industrial waste, and mine wastes) due to logistic and technical barriers [1]. HV waste streams are characterised by a low intrinsic value (high 'place value') and therefore can only be effectively utilised in proximity to their source [8]. Hence, the high transportation costs associated with large volumes of waste further undermine the economic feasibility of material recovery [9]. In addition, conventional resource recovery technologies are prohibitively expensive for these waste streams [10]. Logistical and technical challenges in recovering HV waste flows could impede progress toward responsible consumption and production (SDG 12) [11]. Furthermore, HV waste streams are typically located on former industrial sites, such as abandoned mines and smelting facilities [12], where the health risks of exposure to soil contaminants add another layer of complexity to waste recovery [13]. Moreover, improper HV waste management can contaminate soil and water with heavy metals, harm biodiversity, and disrupt ecological balance [14], challenging SDG 15's goal to reverse land degradation [15].

A new CE approach involves temporarily managing HV waste streams through NbS systems to both recover materials and revitalise degraded landscapes through ecological restoration [1]. This method leverages NbS to concentrate valuable resources until suitable markets emerge, addressing the logistical and technical challenges of HV wastes [7]. A practical approach is the creation of collection hubs to temporarily store materials before final processing at manufacturing facilities, following the analogy of "soil hospitals" used in the Queen Elizabeth Olympic Park soil remediation efforts [16] and deep ground storage of nuclear waste [17].

Accounting for several factors, including economic, environmental, and social considerations [18], is crucial in decision-making processes related to NbS and CE strategies. Each of these dimensions plays a significant role in the overall feasibility and sustainability of the implemented solutions [19]. Economic considerations involve cost-effectiveness, market potential, and long-term economic benefits [20]. Environmental factors encompass the conservation of biodiversity, reduction in greenhouse gas (GHG) emissions, and overall ecosystem health [21]. Social factors include the impact on local communities, job creation, and public health [22]. Determining the most suitable alternative, given multiple objectives, can be achieved with a multi-objective optimisation approach [23,24]. This approach can effectively balance various goals, such as revenues from recovered secondary resources, benefits of NbS ecosystem services, employment opportunities, and reduction in GHG emissions [25]. These goals are sometimes conflicting; for instance, maximising resource recovery might conflict with minimising costs or environmental impacts. Multi-objective optimisation allows for a balanced consideration of these diverse goals, ensuring that the most holistic and beneficial solutions are selected.

The multi-objective optimisation approach must also account for uncertainties due to climate change [26]. Climate change introduces significant variability and unpredictability in environmental conditions such as extreme storms, heatwaves, and altered biogeochemical processes of nutrient cycles, which can affect the performance and outcomes of NbS [27]. Therefore, it is critical to incorporate methods that can handle this uncertainty, ensuring that solutions remain robust and effective under varying future scenarios [28].

2. Previous Works

The discussion above indicates that nature-based secondary resource recovery essentially intersects with three scholarly domains: (1) contaminated land remediation, (2) resource recovery, and (3) nature-based solutions. A recent systematic review found that only a few decision-making frameworks cover at most two domains (remediation and resource recovery or remediation and NbS). The review also highlighted the scarcity of assessing all the sustainability pillars in terms of optimisation objectives, especially in the remediation and resource recovery optimisation literature [29].

2.1. Remediation Domain

Studies have focused on minimising exposure risk to contaminants or geotechnical hazards, as well as remediation costs. For instance, Bayer et al. optimised the groundwater drawdown rate to protect infrastructure in Duisburg, Germany, using a single-objective optimisation model that combines groundwater flow simulation with evolutionary optimisation [30], focusing exclusively on operational aspects. Other works focused on minimising remediation costs in urban brownfield redevelopment [31], social housing on redeveloped brownfields [32], and the bioremediation of chromium-contaminated landfills in India [33].

2.2. Resource Recovery Domain

The literature focuses primarily on maximising revenues from resource recovery. Several waste-to-resource value chains were considered, including organic waste, metal waste, plastic waste, industrial eco-parks, and wastewater treatment. Several studies have examined resource recovery from organic waste, focusing on different aspects, such as the management of the biodegradable fraction of municipal solid waste [34], the national organic waste-to-resource value chain [35,36], and the production of bioenergy through the co-digestion of kitchen waste and rice straw [37]. Similarly, metal waste was explored in the context of strategic support planning for waste electrical and electronic equipment (WEEE) [38]; urban mining of metals, such as scrap iron, non-ferrous waste metals, WEEE, and end-of-life vehicles [39]; location-routing of end-of-life solar photovoltaic panels in the USA [39]; and design optimisation of heap leaching systems within mineral processing [40]. Resource recovery from a wastewater treatment industrial eco-park was examined by a location-routing-network design optimisation model to minimise the total costs of wastewater treatment [41] and was also assessed from an energy-water-waste nexus lens to recover several resources (e.g., biogas, phosphorus, nitrogen, metals, digestate, solid sludge, and microalgae oil) [42].

2.3. NbS Domain

NbS optimisation studies have primarily addressed sustainable stormwater management and wastewater treatment. Several investigations have evaluated sustainable stormwater drainage systems from economic and environmental perspectives, such as a micro-catchment in Costa Rica [43], an urban catchment in St. Maarten in the Caribbean [44], a sub-catchment in São Carlos, Brazil [45], and regional rural-urban catchment planning in the UK [46]. Another study investigated pathways to net zero carbon emissions at the city level by optimising urban land use to maximise carbon sequestration through NbS in Beijing, China, while adhering to urban planning constraints [47]; however, the study did not consider social aspects. Two studies incorporated all the sustainability pillars in the context of SuDS using a Gini coefficient-based optimisation framework [48] and trade-off benefits assessment of green infrastructure [49].

2.4. Interdisciplinary Studies

Few studies have evaluated multiple domains, with contaminated land remediation being the primary focus. Two studies addressed NbS-based remediation, while the other two focused on resource recovery. The first NbS-based study proposed a bi-objective optimisation model to reduce the total nitrogen load at the Tippecanoe River watershed by minimising NbS implementation costs (wetland restoration and buffer strips) [50]. The second study utilised a spatial index system with seven weighted attributes to assess converting brownfields into green infrastructure for ecosystem services like stormwater management and heat island mitigation in Xuzhou, China [51].

The remaining two studies centred on remediation and resource recovery. The first employed a multi-objective optimisation framework with a memetic algorithm to maximise landfill mining profits while minimising carbon emissions and time [52]. The second study

evaluated brownfield redevelopment in the oil industry, using a bi-objective optimisation framework to maximise oil production and minimise the production of water [53].

2.5. Research Gaps and Objectives

While several waste-to-resource value chains were examined in the reviewed literature, none evaluated an NbS resource recovery system or combined resource recovery with soil remediation. Most resource recovery studies focused primarily on economic objectives, often neglecting a holistic sustainability assessment. This economic focus tends to overlook important social and environmental benefits of NbS, such as community involvement, biodiversity enhancement, and climate resilience [54]. Additionally, while all three pillars of sustainability received varying degrees of coverage in the assessed NbS works, economic and environmental objectives were more frequently evaluated. No study has assessed an NbS-based resource recovery system.

Furthermore, few studies have analysed uncertainty explicitly in optimisation. Handling uncertainty in optimisation can be approached through robust optimisation or stochastic optimisation [55]. Robust optimisation aims to find solutions that perform well across a range of possible scenarios, ensuring reliability even under adverse conditions [56]. Stochastic optimisation, on the other hand, involves probabilistic modelling of uncertainties, allowing for solutions that optimise expected outcomes based on the likelihood of different scenarios [57]. For instance, waste generation variability in the organic waste-to-resource context was assessed through a stochastic optimisation framework [35,36], while another study applied a robust optimisation approach for geological uncertainties related to oil brownfield redevelopment [53]. Overlooking the impacts of uncertainties in NbS assessment could undermine the robustness of decision-making analysis outcomes [58].

Given the complexities and uncertainties in recovering HV waste streams through NbS, this study aims to develop a methodological framework to assess the macro-level (national scale) sustainability based on a novel two-stage facility allocation optimisation framework for nature-based secondary resource recovery of HV secondary resources. By integrating robust optimisation to account for long-term climate change projections, the framework ensures solution reliability under various future scenarios. It addresses sustainability by balancing economic, environmental, social, and climate resilience objectives. This study provides a holistic framework for long-term planning in managing HV waste value chains by maximising net profits from resource recovery, enhancing social well-being through increased employment, and minimising climate risks to facilities, thereby advancing alternative circular economy strategies through nature-based resource recovery.

3. Methodology

This section presents the macro-level sustainability assessment framework methodology, starting with the problem statement in Section 3.1. The deterministic and robust mathematical formulations are presented in Sections 3.2 and 3.3, respectively. The solution approach and illustrative case study are outlined in Sections 3.4 and 3.5, while the sensitivity analysis and computational implementation of the optimisation model are described in Sections 3.6 and 3.7.

3.1. Problem Statement

As discussed previously, the natural-based recovery of secondary resources and long-term planning is a complex problem involving the location, allocation, and routing of the various echelons of the resource recovery network while balancing sustainability pillars on a national/regional scale (see Figure 1). The development of a conceptual methodological approach capable of considering multiple stakeholders while handling the uncertainty associated with long-term planning is necessary to assess the sustainability of the secondary resource recovery network and promote temporary waste storage-based CE strategies. The value of HV waste is constrained by geography (longer transportation distances increase transport costs); therefore, the location of HV waste must be taken into account alongside

social and environmental aspects. Additionally, the uncertainties associated with long-term planning (e.g., the impacts of climate change on nature-based systems) must also be considered to ensure the viability of CE strategies for HV waste.

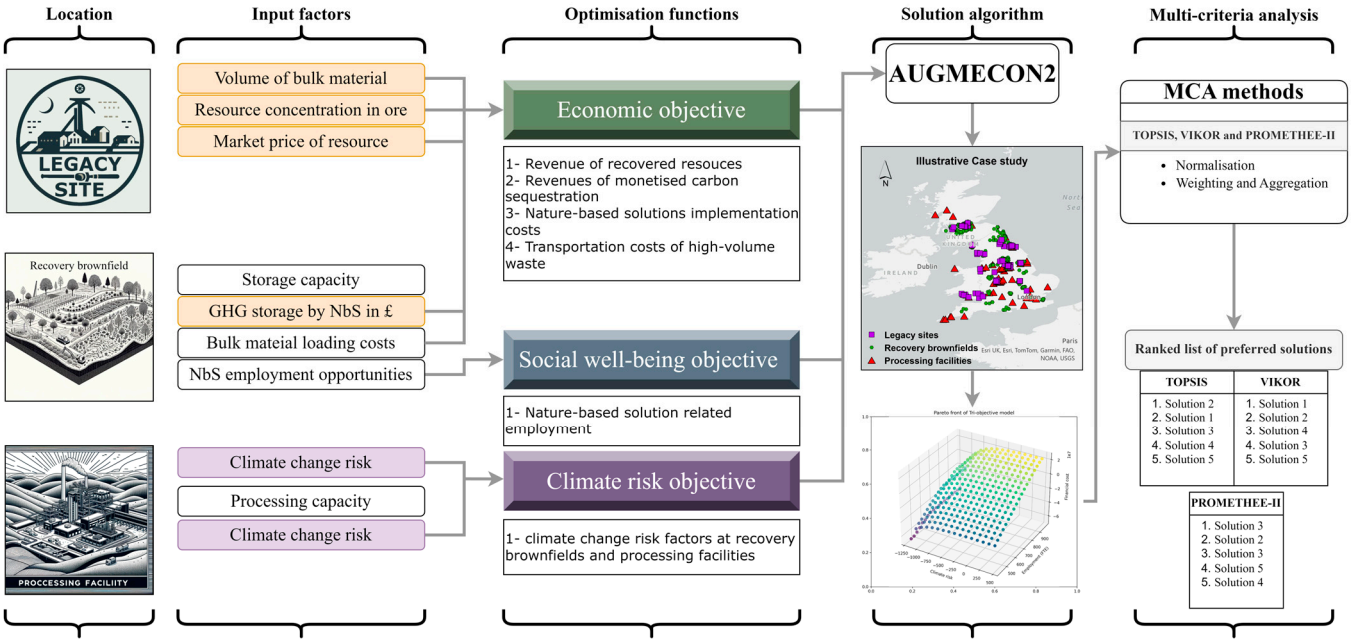

Figure 1. Network schematic of the nature-based secondary resource recovery. The orange-coloured input factors are subject to sensitivity analysis of the deterministic model, whereas the purple-coloured input factors are part of the robust optimisation approach.

3.2. Deterministic Mathematical Formulation

In this paper, we adapted the mixed-integer linear (MILP) deterministic formulation of a two-stage capacitated facility location problem [59] to develop a robust multi-objective optimisation model (see Figure 1). The first objective is to maximise the economic revenues while minimising associated costs. The second objective aims to improve social well-being by maximising NbS-related employment. The third objective aims to minimise the potential risks of climate change on brownfields and processing facilities. The optimisation model is described in the following sections and summarised in Tables A1–A6.

3.2.1. Economic Objective

The first objective in this multi-objective optimisation model aims to maximise the net profit from resource recovery and associated activities. The profit items in the first objective include revenue from the recovery of valuable materials based on their market prices and estimated quantities from legacy sites, as well as revenue from carbon sequestration and storage (CSS) provided by NbS on brownfield sites. The cost items include capital expenditures for implementing NbS, transportation costs for moving materials from legacy sites to brownfields and from brownfields to processing facilities, and the costs associated with loading materials at brownfields for transportation to processing facilities.

$$\begin{aligned} Maximise \sum_{j\in J} \quad & \sum_{k\in K} REV_{rec} \cdot w_{jk} + \sum_{j\in J} REV_{CSS} \cdot period \cdot area_j^{NbS} \cdot y_j \\ & - \sum_{j\in J} CAPEX_{NbS} \cdot area_j^{NbS} \cdot y_j - \sum_{i\in I} \sum_{j\in J} A_{ij} \cdot x_{ij} \\ & - \sum_{j\in J} \sum_{k\in K} B_{jk} \cdot w_{jk} - \sum_{j\in J} \sum_{k\in K} C^{loading} \cdot w_{jk} \end{aligned} \quad (1)$$

where REV_{rec} is the revenue from recovered materials; w_{jk} is a continuous decision variable that denotes the amount of materials transported from brownfield site j to processing facility k; REV_{CSS} is the monetized value of carbon sequestration and storage from NbS; period is the time duration of the project; $area_j^{NbS}$ is the area of NbS implementation at brownfield

j; y_j is a binary variable indicating whether brownfield site j is selected; $CAPEX_{NbS}$ is the capital expense of NbS implementation per hectare; x_{ij} is a continuous decision variable that represents the fraction of materials from legacy site i allocated to brownfield site j; A_{ij} and B_{jk} represent the transportation costs between legacy sites and brownfield sites (A) and from brownfield sites to processing facilities (B), incorporating operational costs of transportation as well as monetised greenhouse gas emissions from transportation per distance unit; and $C^{loading}$ is the loading unit price to load NbS biomass from brownfield j to be transported to processing facility k. The units and values of the parameters are described in Table A7.

3.2.2. Social Well-Being Objective

This objective focuses on maximising social benefits in terms of employment generated by NbS at recovery brownfields.

$$Maximise \sum_{j \in J} EMP_j^{NbS} \cdot area_j^{NbS} \cdot y_j \quad (2)$$

where EMP_j^{NbS} is an employment multiplier per hectare of NbS implementation.

3.2.3. Climate Risk Resilience Objective

This objective aims to minimise climate risk by considering the climate scenarios and their impacts on brownfield and processing facility sites. The objective function is multiplied by -1, so that all the objective functions have the optimisation direction (maximisation) as required by the solution approach.

$$Maximise -1 \times \left(\sum_{j \in J} Ri_j^{climate} \cdot y_j + \sum_{k \in K} Ri_k^{climate} \cdot z_k \right) \quad (3)$$

where $Ri_j^{climate}$ and $Ri_k^{climate}$ are climate risk factors associated with each brownfield site j and processing facility k derived from climate change scenarios.

3.2.4. Constraints

Selection constraints

This constraint limits the number of selected brownfield sites and processing facilities. Exactly N_1 brownfield sites should be selected, while the number of selected processing facilities should be equal to or less than the total number of existing processing facilities (N_2).

$$\sum_{j \in J} y_j = N_1 \quad (4)$$

$$\sum_{k \in K} z_k \leq N_2 \quad (5)$$

Capacity constraints

This constraint ensures that the total volume of materials transported from legacy sites to each brownfield site must not exceed the brownfield site's capacity. S_i represents the volume of materials available at each legacy site i, and c_j is the temporary storage capacity at recovery brownfield j.

$$\sum_{i \in I} s_i \cdot x_{ij} \leq c_j \cdot y_j \quad \forall j \in J \quad (6)$$

This constraint ensures that the total volume of materials processed by each facility must not exceed the facility's capacity. d_k is the processing capacity at a processing facility k.

$$\sum_{j \in j} w_j \cdot x_{ij} \leq d_k \cdot z_k \quad \forall k \in K \quad (7)$$

Flow balance constraint

This constraint ensures that the total volume of materials from legacy sites allocated to a brownfield site equals the volume of materials transported from that brownfield site to processing facilities. This maintains the balance of material flow across the supply chain.

$$\sum_{i \in I} s_i \cdot x_{ij} = \sum_{k \in K} w_{jk} \quad \forall\, k \in K \tag{8}$$

Service constraint

The service constraint ensures that all the material demand from legacy sites is fully serviced by brownfield sites. This constraint mandates that the total amount of materials from each legacy site must be distributed entirely to the brownfield sites.

$$\sum_{j \in J} x_{ij} = 1 \quad \forall\, i \in I \tag{9}$$

Decision variables' constraints

These constraints specify the permissible values and types of the decision variables x_{ij}, w_{jk}, y_j, and z_k, respectively.

$$x_{ij} \in [0,1], \quad \forall\, i \in I, \quad \forall\, j \in J, \tag{10}$$

$$w_{jk} \geq 0 \quad \forall\, j \in J, \ \forall\, k \in K, \tag{11}$$

$$y_j \in \{0,1\}, \ \forall\, j \in J, \tag{12}$$

$$z_k \in \{0,1\}, \ \forall\, k \in K, \tag{13}$$

The following assumptions are made when developing the model:

- All the bulk materials from blast furnaces at legacy sites are collected and recovered.
- Processing facilities have the technological specifications to process all the recoverable resources.

3.3. Robust Mathematical Formulation

To transform the deterministic multi-objective optimisation model into a robust optimisation (RO) model, given that $Ri_j^{climate}$ and $Ri_k^{climate}$ are the only uncertain parameters representing climate change risk indicators, we need to reflect the impact of different climate change scenarios on these parameters. Thus, we consider three climate change scenarios described in [60]:

1. No global mean temperature increases by 2080 (1961–1990 baseline as assumed in UKCP09).
2. Approximately 2 °C global mean temperature increases by 2080.
3. Approximately 4 °C global mean temperature increases by 2080.

Each s $\in$ S will have its own set of values for the climate risk indicators $Ri_j^{climate}$ and $Ri_k^{climate}$.

Given that our objective is to understand how changes in the spatial configuration of recovery brownfields and processing facilities due to climate change might affect the profitability of resource recovery (i.e., the impact of location of the selected sites), we assume that the economic and social well-being factors are not dependent on climate change scenarios. Therefore, we update the climate risk resilience objective to consider the risk indicators under each scenario as follows:

$$Minimise \sum_{j \in J} Ri_j^{climate,s} \cdot y_j + \sum_{k \in K} Ri_k^{climate,s} \cdot z_k \tag{14}$$

where s represents the climate change scenario, namely, p (present), 2c (2 °C increase), and 4c (4 °C increase).

3.4. Solution Approach

The augmented e-constraint method (AUGMECON2) is an efficient multi-objective optimisation algorithm derived from the original AUGMECON method [61] and is designed to handle problems with multiple conflicting objectives [62].

The primary distinction of AUGMECON2 lies in its enhanced ability to reduce the computational burden by avoiding repetitive solutions [63]. AUGMECON2 manages trade-offs between different objectives by prioritizing them, augmenting the objective function with penalty terms, using the epsilon parameter to control surplus variables, and efficiently exploring the solution space to identify a diverse set of Pareto-optimal solutions [63].

$$\text{maximise}\left(f_1(x) + eps \times \left(\frac{S_2}{r_2} + 10^{-1} \times \frac{S_3}{r_3} + \cdots + 10^{-(p-2)} \times \frac{S_p}{r_p}\right)\right) \tag{15}$$

$$\text{Such that} f_2(x) - S_2 = e_2 f_3(x) - S_3 = e_3 \ldots f_{\mathrm{p}}(x) - S_p = e_p \mathrm{x} \in S\mathrm{S_i} \in \mathrm{R}^+ \tag{16}$$

All the e values are the parameters for the right-hand side and all the r values represent the ranges of the corresponding objective functions. Additionally, S values denote the surplus variables. The *eps* is a variable that is limited as $[10^{-6},\ 10^{-3}]$ [63]. An *eps* value of 10^{-3} is assumed in this study.

3.5. Illustrative Case Study

The legacy of the iron and steel industry in the United Kingdom (UK) has resulted in substantial slag deposits scattered across the country. This study leverages the comprehensive database compiled by Riley et al. (2020) [64], which documents the location, volume, and composition of 113 slag deposits in mainland UK (henceforth referred to as legacy sites). These legacy sites represent the supply points in the secondary resource recovery network. We utilised the UK brownfield land spatial dataset, which initially contained 33,710 records. However, the dataset was filtered to exclude data points smaller than 1 hectare and those outside the borough boundaries of the legacy sites. This filtering process resulted in a dataset containing 1302 brownfield candidate sites, which were selected as NbS temporary storage sites for subsequent recovery (henceforth referred to as recovery brownfields). The recovery brownfields represent the first echelon of the two-echelon secondary resource recovery network. The processing facilities of critical materials spatial dataset (59 sites), produced by the UK Critical Minerals Intelligence Centre, were used as the second echelon of the secondary resource recovery network (henceforth referred to as processing facilities). We applied the QGIS network analysis toolbox using the Ordnance Survey's (GB) road network to compute the distance matrix of legacy sites, recovery brownfields, and processing facilities. The profit factors listed in Table 1 were employed to compute the potential profits from recovered materials and monetised GHG sequestration benefits by NbS. The cost factors described in Table 1 were used to calculate the NbS capital expenses, transporting costs, monetised transport GHG emissions, and loading expenses. Social well-being in terms of NbS employment was calculated using NbS employment multipliers. The potential climate change risks were estimated based on three UK climate change scenarios by 2080: present temperature (2016), a 2 °C increase, and a 4 °C increase. The following assumptions are made for the case study:

- The bulk materials' (blast furnace) density is assumed to be 1.5 t/m^3, and around 85% is assumed to be inert materials (i.e., not containing critical materials).
- All the recovery brownfields will be remediated within the 30-year project duration [65].
- Bulk materials will be layered vertically to a depth of 2 m over an area of 1 m^2 on brownfields.
- The recoverable resources are NiO and CoO due to their biomining potential [66,67] and criticality to the UK [68] and EU [69].

- The land value of the remediated recovery brownfields is not considered due to the high variability of real estate value at the national scale [70].
- Exactly $N_1 = 50$ recovery brownfields should be selected, and up to $N_2 \leq 59$ processing facilities can be selected.

Table 1. Case study data sources.

Parameter	Description	Category	Source
Brownfield sites	Locations of brownfields	Spatial data	[71]
Capital expenses of nature-based solutions	Capital expense factor of NbS per unit area	Cost	[46]
Climate change risk indicators spatial dataset	Climate change risk factors per climate change projections	Hydroclimatic data	[60]
Earthmoving cost factors	Loading cost per unit volume	Cost	[72]
Transport GHG emission factor	Carbon emission factors of transport	Cost	[73]
Legacy industrial sites	Locations of legacy industrial sites	Spatial data	[74]
Nature-based solution employment multiplier	Implementation and maintenance phases	Area multiplier	[75]
Passive carbon sequestration by brownfield factor	Carbon sequestered by unit area of brownfields	Area multiplier	[76]
Processing facilities	Locations of processing facilities	Spatial data	[77]
Recoverable resources prices	Low, central, and high estimates	Profit	[78–81]
UK borough boundary lines	Vector dataset of UK roads	Spatial data	[82]
UK road network vector spatial dataset	Vector dataset of UK roads	Spatial data	[83]
Valuation of greenhouse gas emissions	Low, central, and high estimates	Cost	[84]

3.6. Sensitivity Analysis

This section presents the input parameters used in the sensitivity analysis conducted to evaluate the performance of the optimisation model outcomes in terms of computational performance, impacts of variable market dynamics on revenues, and decision-maker preferences.

3.6.1. Number of Grid Points for AUGMECON2

AUGMECON2 requires a grid of points to discretize the range of the objective functions, allowing the method to systematically explore the trade-offs between conflicting objectives [63]. Finding the appropriate grid size is crucial for balancing computational efficiency and accuracy in optimisation problems [61]. It ensures precise representation of the solution space, reduces redundant calculations, avoids weakly optimal solutions, and optimises computational resources usage [85].

To determine the appropriate grid size, we implemented AUGMECON2 with increasing grid sizes of 5×5, 10×10, 20×20, and 30×30 while using central values of cost and revenue factors and climate change risk factors. We then compared the grid sizes in terms of solution time, number of optimal solutions, number of infeasibilities, and number of skipped solutions, as well as the value of the hypervolume indicator. The hypervolume indicator measures the volume of the objective space dominated by a Pareto front approximation, providing a single scalar value (the higher, the better in the case of maximisation problems) that reflects both the convergence and diversity of the solution set [86–88]. A slightly worse than the nadir point is often is selected a reference for maximisation optimisation problems [89]. We assumed the reference points to be less than the nadir point by 1% for CoO and NiO model realisations, as recommended in [90].

3.6.2. Variability in Recovery Revenue, Resource Concentration, and Carbon Pricing

To understand the impacts of operational and market variability on profitability, we conducted a sensitivity analysis on three key factors: resource concentration in ores, market variability of recovered resources, and carbon pricing. Resource concentration reflects the variability in the availability and quality of materials at legacy sites, affecting recovery costs and revenues. Market variability assesses the economic uncertainty of fluctuating prices for recovered materials, impacting the overall financial viability. Carbon pricing examines the monetized benefits of ecosystem services provided by NbS. The ranges of the investigated parameters are presented in Table A7.

3.6.3. Weights of Ranking Methods

In our study, we employed compromise programming to analyse multi-objective Pareto sets. Compromise programming is a multi-objective optimisation method that identifies solutions closest to an ideal point by minimising the distance between the solution and this ideal point within the Pareto front, thus balancing multiple conflicting objectives [91]. To apply compromise programming, we utilized the technique for order of preference by similarity to ideal solution (TOPSIS) and VIKOR and PROMETHEE-II methods [92], which have been used extensively in sustainable engineering applications [93]. These methods are designed to rank and select from a set of alternatives by comparing the distance to an ideal solution, where TOPSIS focuses on the geometric distance. VIKOR incorporates a ranking index based on the closeness to the ideal solution and the maximum group utility [94]. PROMETHEE-II (preference ranking organization method for enrichment evaluations) ranks alternatives based on a pairwise comparison approach, providing a complete ranking of alternatives [95,96]. Recognizing that the weight assigned to each objective can significantly influence the selection of the ideal solution [97], we conducted a sensitivity analysis by varying the weights (i.e., reflecting decision-maker preference) in increments of 10% from 0 to 100% to observe how changes affect the selection of the ideal solution using the following equation:

$$W_{2,3} = \frac{100\% - W_1}{2} \quad (17)$$

where W_1 is the weight of the first objective and $W_{2,3}$ are the weights of the second and third objectives, respectively, with W_2 and W_3 having equal values (e.g., if W_1 is 20%, then W_2 and W_3 would be each 40%). The Spearman's rank correlation and Kendall's Tau tests were used to assess the strength and direction of similarity between the solution rankings by TOPSIS, VIKOR, and PROMETHEE-II, with values close to +1 or -1 indicating a strong positive or negative similarity, and values near 0 indicating little to no similarity [98,99].

3.7. Computational Implementation

In this study, we developed the optimisation model using the Python-based PuLP library [100]. To calculate the origin–destination matrix between legacy sites, recovery brownfields, and processing facilities, we used the QGIS Network Analysis Toolbox 3 with Ordnance Survey (GB) road network data [101] (p. 3). We solved the PuLP-formulated optimisation model with the IBM CPLEX 22.1 solver [102]. The SciPy Python package was employed for statistical analysis of the results [103], while the PYMCDM Python package was used for the multi-criteria [104].

4. Results

This section presents the deterministic model outcomes in Section 4.1, while Section 4.2 analyses the sensitivity analysis results of the deterministic model. The robust optimisation model results are examined in Section 4.3.

4.1. Pareto Sets of AUGMECON2

In this section, we analyse the values of the objective functions across various grid sizes, highlighting the differences in economic, social well-being, and climate change risk minimisation objectives. Tables 2 and 3 show the statistical analysis results that were obtained for CoO and NiO, respectively, across varying grid sizes (5×5, 7×7, 10×10, 15×15, 20×20, 30×30) and three objectives (economic objective, social well-being objective, climate change risk minimisation objective) assuming central values of economic factors (see Figures S1–S6). The results reveal distinct patterns in the data, highlighting differences and similarities between the resources and objectives. For both resources, CoO and NiO, the observed patterns across grid sizes and objectives were consistent.

Table 2. Descriptive statistics of Pareto fronts of CoO for various grid sizes.

Resource	Grid Size	Objective	Mean	Std. Dev.	Min.	Max.	Range
CoO	5×5	Objective 1	-7.97×10^6	1.57×10^7	-3.31×10^7	1.57×10^7	4.88×10^7
	5×5	Objective 2	7.03×10^2	1.36×10^2	5.26×10^2	8.80×10^2	3.54×10^2
	5×5	Objective 3	-3.01×10^2	5.08×10^2	-9.62×10^2	3.59×10^2	1.32×10^3
	7×7	Objective 1	-9.89×10^6	1.78×10^7	-4.39×10^7	1.89×10^7	6.28×10^7
	7×7	Objective 2	7.03×10^2	1.46×10^2	4.92×10^2	9.14×10^2	4.21×10^2
	7×7	Objective 3	-3.01×10^2	5.45×10^2	-1.09×10^3	4.85×10^2	1.57×10^3
	10×10	Objective 1	-1.25×10^7	2.21×10^7	-6.48×10^7	2.08×10^7	8.56×10^7
	10×10	Objective 2	7.03×10^2	1.53×10^2	4.67×10^2	9.39×10^2	4.72×10^2
	10×10	Objective 3	-3.01×10^2	5.72×10^2	-1.18×10^3	5.79×10^2	1.76×10^3
	15×15	Objective 1	-1.97×10^7	4.00×10^7	-1.47×10^8	2.23×10^7	1.69×10^7
	15×15	Objective 2	7.03×10^2	1.59×10^2	4.47×10^2	9.59×10^2	5.11×10^2
	15×15	Objective 3	-3.75×10^2	5.51×10^2	-1.26×10^3	5.06×10^2	1.76×10^3
	20×20	Objective 1	-1.15×10^7	2.10×10^7	-6.51×10^7	2.26×10^7	8.77×10^7
	20×20	Objective 2	7.03×10^2	1.62×10^2	4.38×10^2	9.69×10^2	5.31×10^2
	20×20	Objective 3	-3.56×10^2	5.08×10^2	-1.18×10^3	4.69×10^2	1.65×10^3
	30×30	Objective 1	-1.67×10^7	3.33×10^7	-1.47×10^8	2.28×10^7	1.70×10^8
	30×30	Objective 2	7.03×10^2	1.65×10^2	4.28×10^2	9.78×10^2	5.51×10^2
	30×30	Objective 3	-4.11×10^2	5.08×10^2	-1.26×10^3	4.33×10^2	1.69×10^3

Table 3. Descriptive statistics of Pareto fronts of NiO for various grid sizes.

Resource	Grid Size	Objective	Mean	Std. Dev.	Min.	Max.	Range
NiO	5×5	Objective 1	-5.30×10^6	1.57×10^7	-3.03×10^7	1.83×10^7	4.85×10^7
	5×5	Objective 2	7.03×10^2	1.36×10^2	5.26×10^2	8.80×10^2	3.54×10^2
	5×5	Objective 3	-3.01×10^2	5.08×10^2	-9.62×10^2	3.59×10^2	1.32×10^3
	7×7	Objective 1	-7.21×10^6	1.78×10^7	-4.12×10^7	2.16×10^7	6.28×10^7
	7×7	Objective 2	7.03×10^2	1.46×10^2	4.92×10^2	9.14×10^2	4.21×10^2
	7×7	Objective 3	-3.01×10^2	5.45×10^2	-1.09×10^3	4.85×10^2	1.57×10^3
	10×10	Objective 1	-9.81×10^6	2.21×10^7	-6.21×10^7	2.34×10^7	8.56×10^7
	10×10	Objective 2	7.03×10^2	1.53×10^2	4.67×10^2	9.39×10^2	4.72×10^2
	10×10	Objective 3	-3.01×10^2	5.72×10^2	-1.18×10^3	5.79×10^2	1.76×10^3
	15×15	Objective 1	-1.71×10^7	4.00×10^7	-1.45×10^8	2.49×10^7	1.70×10^8
	15×15	Objective 2	7.03×10^2	1.59×10^2	4.47×10^2	9.59×10^2	5.11×10^2
	15×15	Objective 3	-3.75×10^2	5.51×10^2	-1.26×10^3	5.06×10^2	1.76×10^3
	20×20	Objective 1	-8.80×10^6	2.10×10^7	-6.24×10^7	2.53×10^7	8.77×10^7
	20×20	Objective 2	7.03×10^2	1.62×10^2	4.38×10^2	9.69×10^2	5.31×10^2
	20×20	Objective 3	-3.56×10^2	5.08×10^2	-1.18×10^3	4.69×10^2	1.65×10^3
	30×30	Objective 1	-1.40×10^7	3.32×10^7	-1.45×10^8	2.55×10^7	1.70×10^8
	30×30	Objective 2	7.03×10^2	1.65×10^2	4.28×10^2	9.78×10^2	5.51×10^2
	30×30	Objective 3	-4.11×10^2	5.08×10^2	-1.26×10^3	4.33×10^2	1.69×10^3

The economic objective exhibited the highest variability, with large standard deviations and ranges for all the grid sizes. The mean values for the economic objective were significantly negative, increasing in magnitude with larger grids, indicating a considerable negative skew. For instance, the mean for CoO ranged from approximately £-7.97×10^6 (5×5) to £-1.97×10^7 (15×15), with the range increasing from £4.88×10^7 to £1.70×10^8. Similar trends were observed for NiO, with mean values ranging from £-5.30×10^6 to £-1.71×10^7 and the range increasing from £4.85×10^7 to £1.70×10^8.

The social well-being objective (objective 2) demonstrated minimal variability across all the grid sizes for both resources. The mean values remained consistently around 702–703,

with small standard deviations and ranges. This stability suggests that objective 2 is less affected by changes in grid size compared to the economic objective and climate change risk minimisation objective. Although the standard deviation and range for objective 2 increased slightly with the grid size, the increase was not as pronounced as for the economic objective.

The climate change risk minimisation objective (objective 3) showed moderate variability, with mean values ranging from −300 to −400. The range of objective 3 increased with the grid size, indicating higher variability in larger grids. For CoO, the mean values ranged from £-3.01×10^2 (5×5) to £-4.11×10^2 (30×30), and the range increased from £1.32×10^3 to £1.76×10^3. NiO exhibited similar trends, with mean values ranging from £-3.01×10^2 to £-4.11×10^2 and the range increasing from £1.32×10^3 to £1.76×10^3.

Overall, the analysis reveals that the economic objective is characterised by high variability and extreme negative mean values, especially as the grid size increases. The social well-being objective remains stable across all the grid sizes, showing minimal variability. Objective 3, while demonstrating moderate variability, also shows an increased range with larger grid sizes, indicating more variability in larger grids.

4.2. Sensitivity Analysis

This section presents the sensitivity analysis results, evaluating the optimisation model outcomes in terms of AUGMECON2 computational performance, revenues under variable market dynamics, and decision-maker preferences.

4.2.1. AUGMECON2 Performance Sensitivity to Grid Size

In this section, we varied the grid size of AUGMECON2 to investigate the model performance and the characteristics of the Pareto fronts.

Table 4 shows the sensitivity analysis results of the AUGMECON2 grid size in terms of the number of optimal solutions, infeasibilities (i.e., no optimal solutions were found), skipped solutions (i.e., redundant iterations), hypervolume indicator (HV), and solution time. We noticed that the choice of the recoverable resource did not affect the solutions' numerical characteristics (e.g., number of optimal solutions), as they were identical in both the CoO and NiO model runs.

Table 4. Sensitivity analysis results of AUGMECON2 grid size.

	Grid Size					
CoO	**5 × 5**	**7 × 7**	**10 × 10**	**15 × 15**	**20 × 20**	**30 × 30**
Optimal solutions	16	36	81	182	304	696
Infeasibilities	4	6	9	14	38	58
Skipped solutions	5	7	10	29	58	146
Hypervolume	9.279×10^{15}	1.083×10^{16}	1.248×10^{16}	1.423×10^{16}	1.482×10^{16}	2.088×10^{16}
Solution time (s)	1324	2468	5220	11,754	14,368	47,881
NiO	**5 × 5**	**7 × 7**	**10 × 10**	**15 × 15**	**20 × 20**	**30 × 30**
Feasible solutions	16	36	81	182	304	696
Infeasibilities	4	6	9	14	38	58
Skipped solutions	5	7	10	29	58	146
Hypervolume	9.366×10^{15}	1.093×10^{16}	1.259×10^{16}	1.435×10^{16}	1.482×10^{16}	2.100×10^{16}
Solution time (s)	1006	3019	5574	12,927	14,086	32,403

However, the HV indicator values were slightly different due to variations in reference points, which differ because the first objective value depends on the revenues of recovered materials. The HV values for grid sizes (10×10) to (20×20) were close to those of the 5×5 grid size. Therefore, we introduced the 7×7 grid size to determine if a satisfactory HV value could be obtained in a shorter solution time. Considering that AUGMECON2 is an exact solution approach and the large size of the employed case study (113 legacy

sites, 1302 recoverable brownfields, and 59 processing facilities), we determined that the 7 × 7 grid size offers an ideal trade-off between adequate resolution of the Pareto and solution time (2468–3019 s). For comparison of location–allocation–routing optimisation literature, a heuristics approach solved an 81-nodes two-echelon network multi-objective optimisation approach in 251 s [105], while a metaheuristics approach achieved solution times of 364–602 s for a 30–25–125 network transportation–location–routing tri-objective optimisation problem [106].

4.2.2. Variability in Recovery Revenue, Resource Concentration, and Carbon Pricing

In this section, we examine the impact of market price and resource concentration of CoO and NiO in ores, as well as the monetised carbon storage and sequestration (CSS) benefits of NbS. Figure 2 presents box plots of the sensitivity analysis results concerning market price and concentration of the recovered resource. Observing the box plots of the minimum resource concentration in Figure 2a,b, we found that they are identical regardless of the market price estimates. This is because the minimum concentration is indeed zero, as reported in [74]; hence, the positive values in the box plots represent the monetised carbon sequestration by NbS.

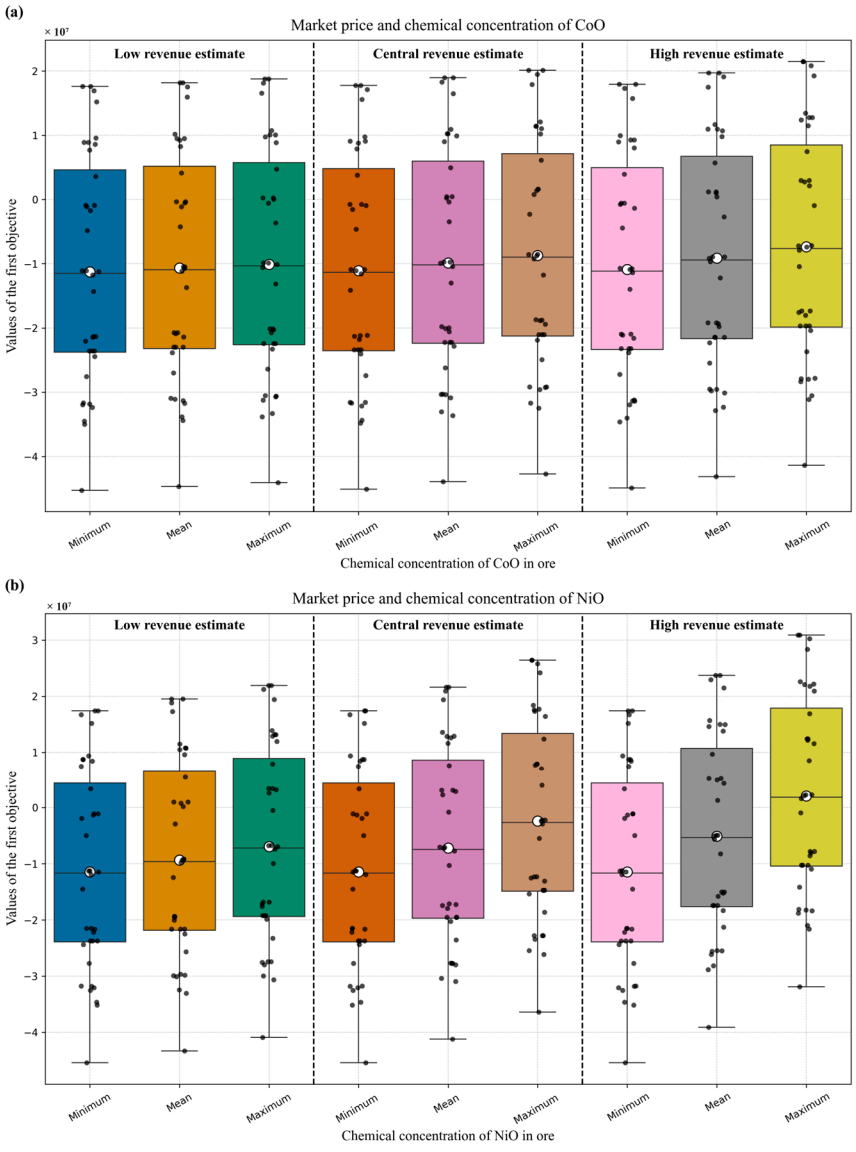

Figure 2. Sensitivity analysis results of market price of recovered materials vs. resource concentration in ore: (**a**) CoO, (**b**) NiO.

In the case of mean and high concentrations, the differences between central and high market prices of CoO are minor, while they are more pronounced for NiO. For example, in Figure 2b, the upper whisker of the box plot for high market price and high concentration of NiO is significantly higher than the other box plots. Additionally, comparing Figure 2a,b reveals that the overall revenues of NiO are higher than those of CoO across all the market price estimates. This difference stems from the higher range of the assumed market prices for NiO compared to CoO.

It was also important to consider the sensitivity of the overall revenues to changes in the monetisation factor of the carbon sequestration and storage (CSS) by the implemented NbS. Figure 3 presents the sensitivity analysis results of the monetised CSS benefits and market prices of the recovered resources. Observing the blue-dotted horizontal line in Figure 3a,b, which represents the breakeven line (i.e., profitability vs. losses), we noted that the low CSS estimate simulations did not yield profitable solutions for either CoO or NiO. In the case of the central CSS estimate, while some solutions (i.e., spatial configuration of the recovery brownfields and processing facilities) are profitable, the mean of the solutions across all the chemical concentrations of CoO and NiO are below the breakeven line. On the other hand, the high CSS simulations produced a higher number of profitable spatial configurations regardless of the chemical concentration level, suggesting that the profitability of the nature-based secondary resources is highly sensitive to the monetary estimation of the ecosystem services generated by NbS.

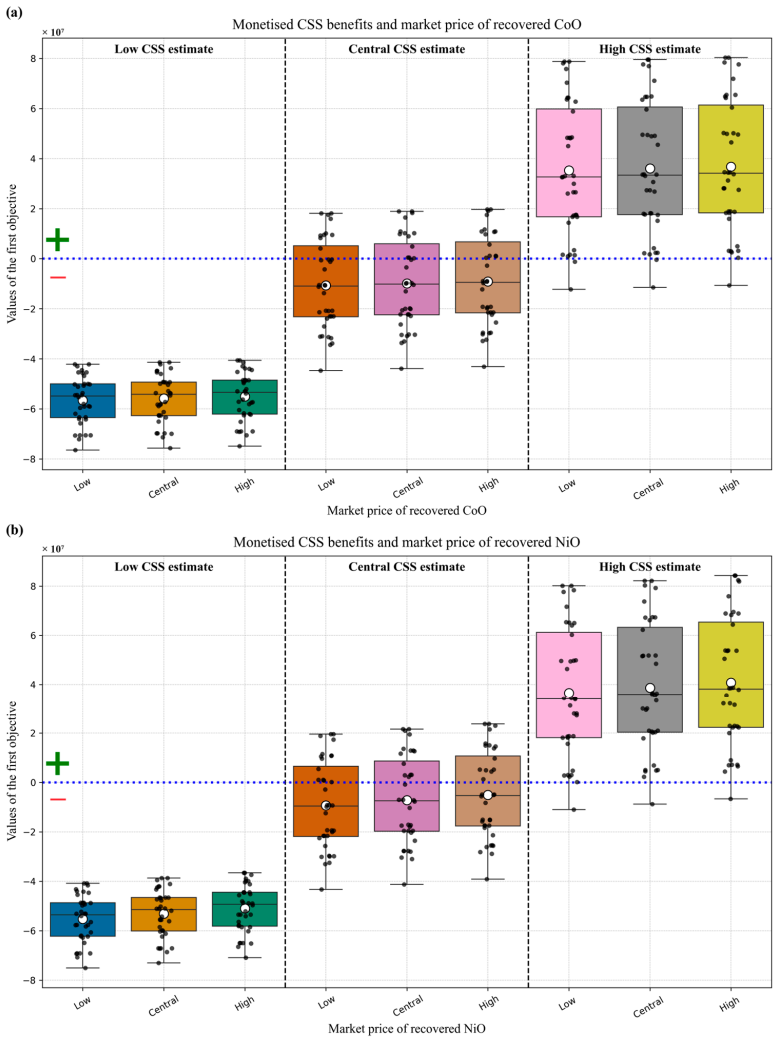

Figure 3. Sensitivity analysis results of monetised carbon storage benefits by NbS vs. market price of recovered materials: (**a**) CoO, (**b**) NiO.

4.2.3. Multi-Criteria Analysis of Pareto Sets: Compromise Programming

In this section, we investigate the sensitivity of solution outranking to weights used in TOPSIS, VIKOR, and PROMETHEE-II. The weights were varied in increments of 10% for the economic, social, and climate risk objectives, ranging from 10% to 100%, with equal weighting for the remaining two objectives. The Spearman and Kendall Tau coefficients were applied to assess the similarity of the rankings produced by TOPSIS, VIKOR, and PROMETHEE-II. Figure 4a,b depict the correlation coefficients for both CoO and NiO, respectively, across the range of weights (10–100%) for each objective. We observe high positive correlations, ranging from 0.86 to 1.0, across all weights, indicating a high similarity of TOPSIS, VIKOR, and PROMETHEE-II rankings, with almost perfect similarity at higher weights of 70–100%. These findings corroborate similar observations in the literature [107] and suggest that the solutions produced are robust to a wide range of decision-maker preferences [108].

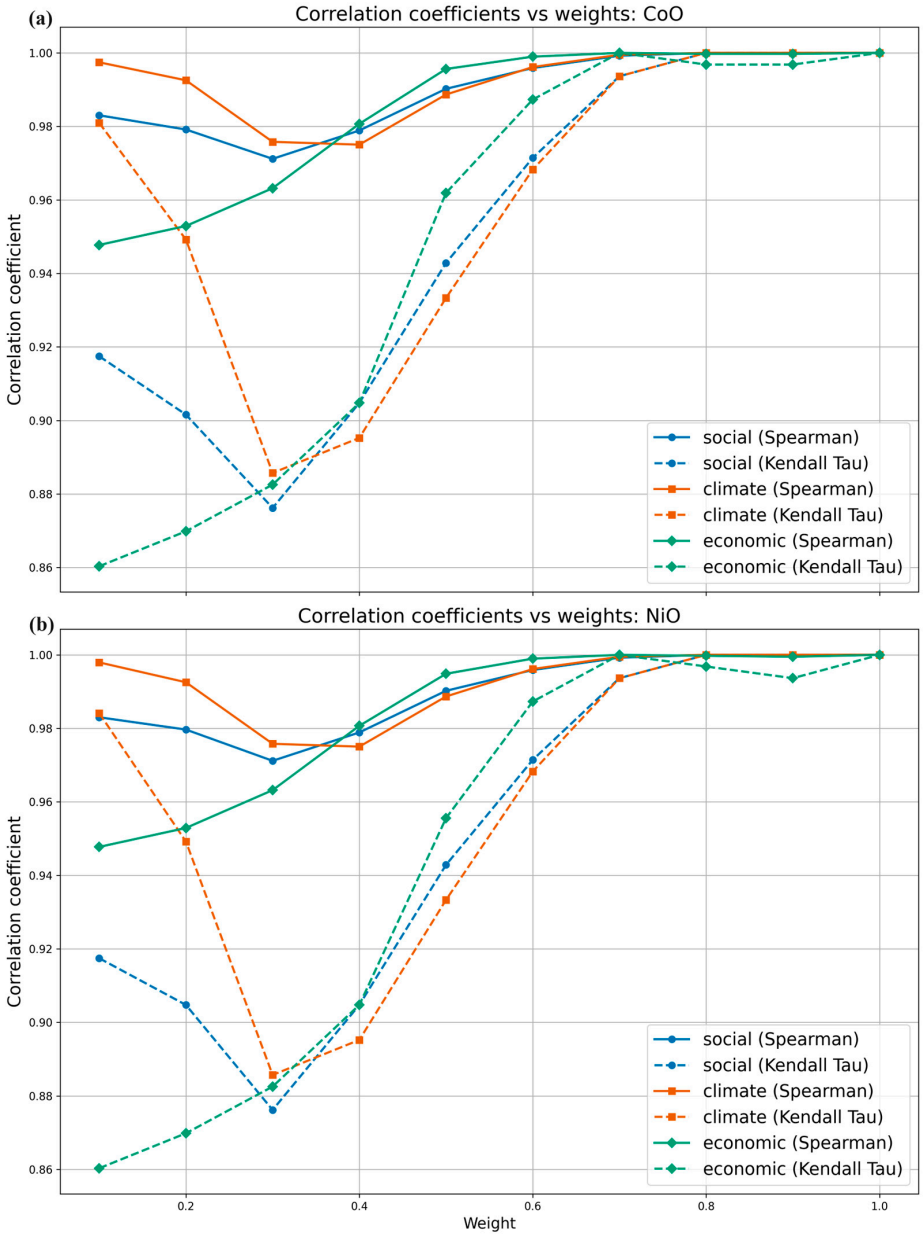

Figure 4. Correlation coefficients of varying objective's weight for TOPSIS, VIKOR, and PROMETHEE-II: (**a**) CoO, (**b**) NiO.

TOPSIS, VIKOR, and PROMETHEE-II are often used to select an optimal solution from the Pareto front by weighting each objective based on decision-maker preferences (see Tables S1–S6 for ranking outcomes). Figure 5 shows the Pareto front of the optimisation model, where the optimal solutions are highlighted with 'x' markers in blue, lime, and red (assuming 100% weight for each), illustrating the trade-offs among the objectives.

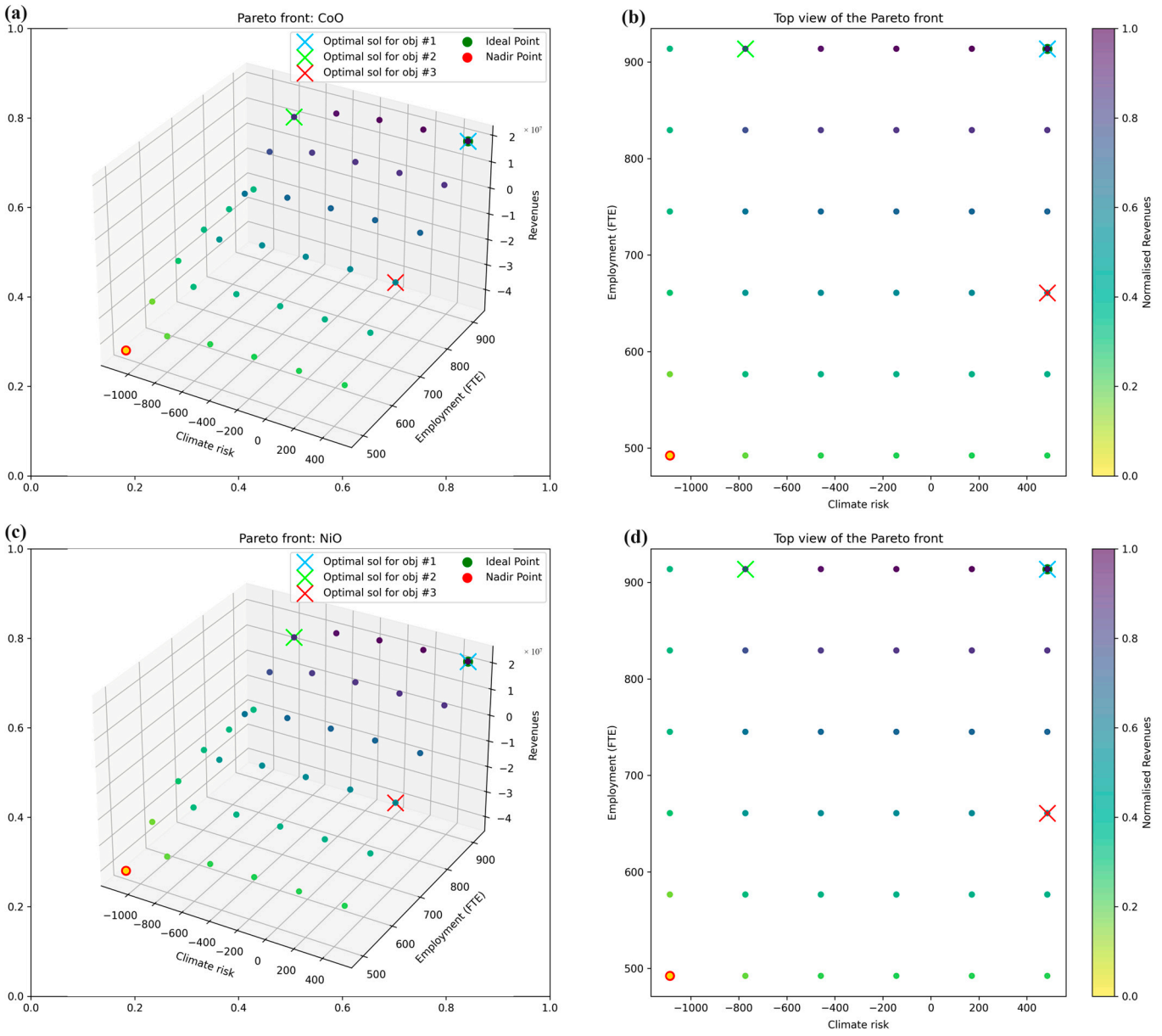

Figure 5. Pareto front of the optimisation model: (**a**) 3D view of CoO, (**b**) top view of CoO, (**c**) 3D view of NiO, (**d**) top view of NiO.

Examining Figure 5a,c, we observe that the selected optimal solutions for both CoO and NiO are similar, indicating that the value of the objective functions is significantly sensitive to the spatial configuration of the resource recovery network rather than the economic factors of the model. Furthermore, examining the TOPSIS, VIKOR, and PROMETHEE-II rankings in Tables S1–S6, we notice that certain solutions frequently appear as optimal for all the objectives. This suggests that a subset of the Pareto front (solutions 31–37) contains the most preferred solutions. Therefore, this subset could be analysed further for additional insights (e.g., the optimal solutions could be presented in a map similar to Section 3.3) [109].

4.3. Robust Optimisation of Climate Change Uncertainty

In this section, we analyse the results of a robust optimisation model under three climate change scenarios projected for 2080 (i.e., present temperatures remain unchanged, a 2 °C increase, and a 4 °C increase). Figure 6a–c present the values of the objective functions for CoO and NiO across the climate change scenarios. Figure 6a depicts the value of the first objective function (maximising revenues). It is immediately noticeable that the revenues from recovering CoO and NiO remain constant across all the climate change scenarios, indicating that the optimal solutions are robust to climate change uncertainties. A similar observation is seen in Figure 6b, which shows that full-time NbS-related employment is robust to climate change uncertainty and remains consistent regardless of the choice of recoverable resource due to the assumed NbS employment multiplier. Figure 6c displays the climate change risk factors for both CoO and NiO across climate change scenarios. It is apparent that the climate risk factors are similar for both CoO and NiO, suggesting that the value of the climate risk minimisation objective is not sensitive to the choice of recoverable resource.

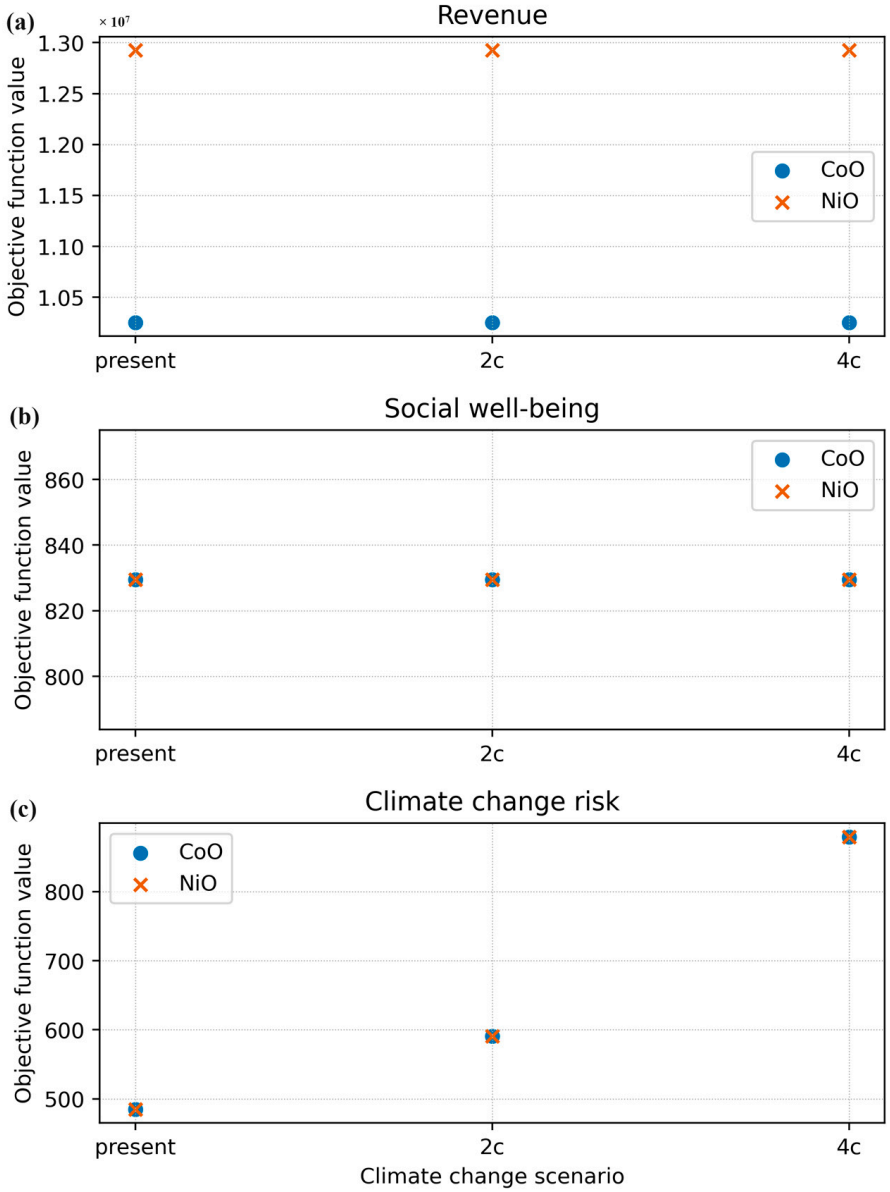

Figure 6. Objective function values of optimal solutions across climate change scenarios: (**a**) economic objective, (**b**) social well-being objective, (**c**) climate change risk.

The selected recovery brownfields and processing facilities for each optimal solution across the climate change scenarios are illustrated in Figures S5–S7 for CoO and Figures S8–S10 for NiO. Figures S5–S7 represent the present, 2 °C, and 4 °C climate change scenarios for CoO, respectively. Upon examining the first objective maps of CoO in Figures S1–S3, it is apparent that the spatial configuration for the optimal solution of the first objective is the same for all the climate scenarios (i.e., the selected recovery brownfields and processing facilities are robust to climate change uncertainty when optimised to maximise revenues). The spatial configuration of the optimal solutions for the social well-being objective was identical for the 2 °C and 4 °C climate change projections, whereas the present temperature scenario was slightly different. In the case of the climate risk minimisation objective, the selected recovery brownfields and processing facilities were geographically similar for the 2 °C and 4 °C scenarios but showed some variation for the present temperature scenario.

In the case of NiO, Figures S8–S10 represent the present, 2 °C, and 4 °C climate change scenarios, respectively. The spatial configuration of the optimal solutions for the first objective and third objective was identical across the climate change scenarios, as shown in Figures S4–S6. However, the spatial configurations for maximising NbS-related employment (2nd objective) were slightly different between the present temperature and 2 °C and 4 °C scenarios, with minor variations located in western Scotland and northeast and southeast England.

The comparison of the CoO and NiO maps across the climate change scenarios revealed that the spatial configurations for the first objective were identical in both cases. For the second objective, the selected sites in CoO and NiO were similar for the present temperature scenarios but showed slight differences in the 2 °C and 4 °C scenarios. For the climate change risk minimisation objective (3rd objective), the selected sites for NiO and CoO were slightly different for the present and 4 °C scenarios, particularly in northeast England, whereas a higher degree of variation was observed in the 2 °C scenario.

5. Discussion

In this section, we discuss the performance of the AUGMECON2 algorithm and the implications of resource value and carbon pricing on the economic objectives, as well as the impact of decision-maker preferences and robust optimisation under climate change uncertainty.

5.1. Performance of AUGMECON2

The performance of the AUGMECON2 algorithm in addressing a tri-objective location–allocation–routing optimisation of nature-based resource recovery was tested, focusing on the impact of grid points in achieving an optimal balance between solution quality and computational efficiency. As noted in Section 4.2.1, the solution times and HV values were considered reasonable given the conceptual purpose of the paper, the number of optimisation objectives, and the case study size (national level). That said, the AUGMECON2 approach might not be able to generate a higher-resolution Pareto front or handle additional objectives or more scenarios (e.g., alternative transport modes) within reasonable solution times. Therefore, future efforts might consider using novel exact solution approaches, such as the AUGMECON-R [85], or metaheuristics approaches, such as NSGA-III [110] or memetic algorithms (i.e., combining evolutionary algorithms with local search) for larger data instances [52,111]. The comparison of several solution approaches is recommended to enhance robustness, improve convergence, and provide a more diverse and high-quality set of solutions for complex location–allocation–routing optimisation problems [112].

5.2. Impacts of Resource Value and Carbon Pricing

The sensitivity of the economic objective function (i.e., revenue) to three relevant input factors was analysed in Section 4.2.2. The economic-related factors included the market price of recovered resources, the chemical concentration of resources in ore, and the

carbon pricing of carbon sequestration by NbS. The revenue sensitivity to market price and chemical concentration of resources was analysed first. The results suggested that revenues were more sensitive to the market price of recovered resources, with slight variations in sensitivity based on the price range of the recovered resource.

Considering that the revenue from recovered resources also depends on the recovery efficiency of the nature-based system, a conservative assumption was made in Section 3.2.4 that only 15% of the bulk material contained recoverable compounds (i.e., 85% of the bulk materials are assumed to be inert). Therefore, revenues are likely to increase with more efficient nature-based secondary resource recovery systems. Additionally, the current model did not account for the recovery of multiple secondary resources, such as ferrous metals or cleaned aggregates reused in construction, which is more realistic based on existing conventional primary mining supply chains. Furthermore, the results suggest that revenues from secondary resources recovery alone do not support the economic feasibility, corroborating previous findings [9].

Therefore, a coupled resource recovery–land remediation NbS is considered, in addition to natural capital accounting of NbS systems. In this study, we only considered one ecosystem service: carbon sequestration and storage by NbS. The sensitivity analysis results of resource market pricing and carbon pricing in Figure 3 indicate that revenues were more sensitive to carbon pricing, assuming the same amount of carbon dioxide was sequestered in all the cases. Given the potentially large scale and long-time horizons of such projects, additional ecosystem services and disservices (e.g., non-edible crop provision or harmful impacts on biodiversity) should be considered using varying discount rates to generate a diverse range of likely solution sets that are robust to market dynamics.

5.3. Impact of Decision-Maker Preferences on Selected Solutions

The Pareto front of multi-objective optimisation represents the trade-offs among the optimisation objectives; therefore, ranking methods are employed to prioritize the solutions by weighting each objective based on the decision-maker's preferences or priorities. The sensitivity of solution rankings to objective weighting was presented in Section 4.2.3. The high correlation coefficient of the solution rankings indicated that the optimal solutions are robust to a wide range of decision-maker preferences. Ranking methods are useful for exploring the solution space to identify the most optimal subset of solutions for further analysis. For instance, solutions 31–37 appeared most frequently with higher weights across all the optimisation objectives (see Tables S1–S4), suggesting that a specific set of recovery brownfield's locations offers the best trade-off among all the optimisation objectives, and further planning efforts could be focused on these regions.

Although a wide range of weights was assessed in this work, in practice, the weights should be assigned based on expert judgement or a consensus-building process [113,114]. Future efforts should consider additional criteria to reflect the values and concerns of a broader spectrum of stakeholders, typical of national-scale projects. Additionally, TOPSIS, VIKOR, and PROMETHEE-II were used in this study to rank the solutions; further ranking methods could be employed to mitigate the risk of any single method's bias disproportionately influencing the selection of the optimal solution [115]. Finally, the weights are inherently subjective and sometimes difficult to obtain [116]. Hence, fuzzy ranking methods could be utilised to handle the uncertainty of weights and offer a more nuanced selection of optimal solutions [117,118].

5.4. Robust Optimisation under Climate Change Uncertainty

The aim of the RO employed in this paper was to guide macro-level sustainability decision-making for nature-based secondary resource recovery from legacy industrial sites under climate change uncertainty. The results of the RO indicate that the proposed solutions maintain their performance despite the variations in climate change projections, indicating the robustness and reliability of the solution set. Therefore, adopting an RO approach can provide designers and decision-makers insights to design and implement NbS-based

circular economy strategies that are not only economically viable but also resilient to future climate scenarios. This ensures HV does not remain overlooked as a potential source of revenue and mitigates the environmental risks associated with legacy industrial sites. Moreover, the RO results could help decision-makers shift from a reactive, business-as-usual mindset to a forward-looking perspective [119], enabling the development of climate-aware regional NbS CE strategies for HV waste.

In this study, a static RO approach (now-and-then) was implemented that considered the worst-case scenario within a predefined discrete uncertainty set [55], focusing on one uncertain parameter related to climate change risks. While this approach provides valuable insights, additional uncertainties should be considered in future works, such as resource concentration (demand uncertainty), economic factors like transportation costs, and operational uncertainties, such as uncertain capacities in processing facilities and occupational safety considerations. Furthermore, future efforts could benefit from applying a two-stage optimisation approach that combines robust and stochastic methods to manage multiple uncertainties for complex problems by balancing adaptability and computational feasibility [120].

6. Conclusions

The aim of this paper was to propose a robust multi-objective optimisation framework to assess the sustainability and enable the nature-based secondary resource recovery of HV waste under climate change uncertainty. Using an illustrative national-scale case study of legacy mining waste, this research developed a multi-objective mixed-integer linear programming to optimize economic revenues and social well-being and minimise climate change risks using an exact solution approach.

The main findings of this illustrative case study indicate that NbS could significantly enhance the economic feasibility of HV waste management by incorporating carbon sequestration benefits and generating employment. The optimisation results demonstrate the resilience of NbS-based strategies despite climate change variations. Additionally, while NbS can improve the circularity potential of HV waste nationally, it is crucial to consider additional ecosystem services and uncertainties for effective macro-level sustainability. The proposed framework provides valuable insights for policymakers and stakeholders in developing regional and national nature-based circular economy strategies for HV waste streams.

Supplementary Materials: The following supporting information can be downloaded at: https://www.mdpi.com/article/10.3390/su16167220/s1, Table S1. Top 5 solutions TOPSIS, VIKOR, and PROMETHEE-II rankings: CoO under the present climate change projection. Table S2. Top 5 solutions TOPSIS, VIKOR, and PROMETHEE-II rankings: CoO under the 2 °C climate change projection. Table S3. Top 5 solutions TOPSIS, VIKOR, and PROMETHEE-II rankings: CoO under the 4 °C climate change projection. Table S4. Top 5 solutions TOPSIS, VIKOR, and PROMETHEE-II rankings: NiO under the present climate change projection. Table S5. Top 5 solutions TOPSIS, VIKOR, and PROMETHEE-II rankings: NiO under the 2 °C climate change projection. Table S6. Top 5 solutions TOPSIS, VIKOR, and PROMETHEE-II rankings: NiO under the 4 °C climate change projection. Figure S1. Pareto front of CoO assuming central economic factors: (a) 5 × 5 grid size, (b) 7 × 7 grid size, (c) 10 × 10 grid size. Figure S2. Pareto front of CoO assuming central economic factors: (a) 15 × 15 grid size, (b) 20 × 20 grid size, (c) 30 × 30 grid size. Figure S3. Pareto front of NiO assuming central economic factors: (a) 5 × 5 grid size, (b) 7 × 7 grid size, (c) 10 × 10 grid size. Figure S4. Pareto front of NiO assuming central economic factors: (a) 15 × 15 grid size, (b) 2 × 20 grid size, (c) 30 × 30 grid size. Figure S5. Maps of the optimal solutions for CoO: present temperature scenario. Figure S6. Maps of the optimal solutions for CoO: 2 °C scenario. Figure S7. Maps of the optimal solutions for CoO: 4 °C scenario. Figure S8. Maps of the optimal solutions for NiO: present temperature scenario. Figure S9. Maps of the optimal solutions for NiO: 2 °C scenario. Figure S10. Maps of the optimal solutions for NiO: 4 °C scenario.

Author Contributions: Conceptualization, K.A., D.S., M.H., and P.C.; methodology, K.A. and M.B.; software, K.A. and M.B.; data curation, K.A.; formal analysis, K.A.; investigation, K.A.; validation, K.A. and M.B.; visualisation, K.A; writing—original draft preparation, K.A.; writing—review and editing, K.A., M.B., D.S., M.H. and P.C; supervision, D.S., M.H. and P.C.; project administration, P.C. All authors have read and agreed to the published version of the manuscript.

Funding: The work was partly supported by the Engineering and Physical Sciences Research Council, UK (grant numbers: EP/T03100X/1).

Institutional Review Board Statement: Not applicable.

Informed Consent Statement: Not applicable.

Data Availability Statement: The data used are derived from public sources.

Acknowledgments: The authors are grateful to the Deanship of Scientific Research at the University of Bisha for the financial support of the first author through the Scholarship Program of the University.

Conflicts of Interest: The authors declare no conflicts of interest.

Appendix A

Table A1. Sets of the optimisation model.

Set	Description
I	Set of legacy sites where materials are available.
J	Set of recovery brownfield sites available for nature-based solutions.
J	Set of processing facilities available for final processing of materials.
K	Set of climate change scenarios.

Table A2. Input parameters of the optimisation model.

Parameter	Description
REV_{rec}	Revenue from recovered materials based on market prices.
REV_{CSS}	Monetised value of carbon sequestration and storage from NbS.
$CAPEX_{NbS}$	Capital expense for NbS implementation per hectare.
A_{ij}	Transportation cost from legacy site i to brownfield site j.
B_{jk}	Transportation cost from brownfield site j to processing facility k.
$C^{loading}$	Loading cost for materials at brownfields for transportation.
EMP_j^{NbS}.	Employment multiplier per hectare of NbS implementation at brownfield j.
$Ri_j^{climate}$	Climate risk factor for brownfield site j.
$Ri_k^{climate}$	Climate risk factor for processing facility k.
s_i	Volume of materials available at legacy site i.
c_{j}	Temporary storage capacity at brownfield site j.
d_k	Processing capacity at processing facility k.
period	Duration of the project.
N_1	Number of brownfield sites to be selected.
N_2	Maximum number of processing facilities that can be selected.

Table A3. Decision variables of the optimisation model.

Variable	Description
x_{ij}	Continuous variable representing the fraction of materials from legacy site iii allocated to brownfield site j.
w_{jk}	Continuous variable representing the amount of materials transported from brownfield site j to processing facility k.
y_j	Binary variable indicating whether brownfield site j is selected.
z_k	Binary variable indicating whether processing facility k is selected.

Table A4. Deterministic mathematical formulation.

Objective	Description
Economic objective	$Maximise \sum_{j\in J} \sum_{k\in K} REV_{rec} \cdot w_{jk} + \sum_{j\in J} \sum_{k\in K} REV_{CSS} \cdot period \cdot area_j^{NbS} \cdot y_j - \sum_{j\in J} CAPEX_{NbS} \cdot area_j^{NbS} \cdot y_j - \sum_{i\in I} \sum_{j\in J} A_{ij} \cdot x_{ij} - \sum_{j\in J} \sum_{k\in K} B_{jk} \cdot w_{jk} - \sum_{j\in J} \sum_{k\in K} C^{loading} \cdot w_{jk}$
Social well-being objective	$Maximise \sum_{j\in J} EMP_j^{NbS} . area_j^{NbS} . y_j$
Climate risk resilience objective	$Maximise -1 \times \left(\sum_{j\in J} Ri_j^{climate} \cdot y_j + \sum_{k\in K} Ri_k^{climate} \cdot z_k\right)$

Table A5. Robust mathematical formulation.

Objective	Description
Robust climate risk resilience objective	$Minimise \sum_{j\in J} Ri_j^{climate,s} \cdot y_j + \sum_{k\in K} Ri_k^{climate,s} \cdot z_k$

Table A6. Constraints of the optimisation model.

Constraint	Description
Selection constraint (1)	Exactly $N_1 = 50$ brownfield sites should be selected : $\sum_{j\in J} y_j = N_1$
Selection constraint (2)	The number of selected processing facilities should be at most $N_2 = 59$: $\sum_{k\in K} z_k \leq N_2$
Capacity constraint (1)	The total volume of materials transported to each brownfield site must not exceed its capacity: $\sum_{i\in I} s_i \cdot x_{ij} \leq c_j \cdot y_j \forall j \in J$
Capacity constraint (2)	The total volume of materials processed by each facility must not exceed its capacity: $\sum_{j\in j} w_j \cdot x_{ij} \leq d_k \cdot z_k \forall k \in K$
Flow balance constraint	Ensure material flow balance from legacy sites through brownfields to processing facilities $\sum_{i\in I} s_i \cdot x_{ij} = \sum_{k\in K} w_{jk} \quad \forall k \in K$
Service constraint	Ensure all material from legacy sites is allocated to brownfield sites: $\sum_{j\in J} x_{ij} = 1 \quad \forall i \in I$
Decision variable constraint (1)	Decision variable x_{ij} must be between 0 and 1 : $x_{ij} \in [0,1], \quad \forall i \in I, \quad \forall j \in J$
Decision variable constraint (2)	Decision variable w_{jk} must be non − negative : $w_{jk} \geq 0 \quad \forall j \in J, \forall k \in K$
Decision variable constraint (3)	Binary decision variable $y_j : y_j \in \{0,1\}, \forall j \in J$
Decision variable constraint (4)	Binary decision variable z_k: $z_k \in \{0,1\}, \forall k \in K$

Table A7. The Economic, social, and environmental factors used in this study.

Parameter	Low	Central	High	Unit	Source
Capital expenses of nature-based solutions	n.a. *	123	n.a.	GBP/hectare	[46]
Earth-moving cost factor (*a 1 m^3 crawler assuming 10 loadings per hour*)	n.a.	26.84	n.a.	GBP/hour	[72]
Transport GHG emission factor (assuming average laden rigid lorry)	n.a.	0.9635	n.a.	$kgCO_2e$/km	[73]
Nature-based solution employment multiplier (implementation phase)	n.a.	0.04	n.a.	Full-time equivalent/hectare/year	[75]
Nature-based solution employment multiplier (maintenance phase)	n.a.	0.01	n.a.	Full-time equivalent/hectare/year	[75]
Passive carbon sequestration by brownfield factor	n.a.	4	n.a.	tCO_2e/hectare	[76]
Recoverable resources prices (CoO)	2000	4500	6000	GBP/ton	[78,79]
Recoverable resources prices (NiO)	2500	5000	7500	GBP/ton	[80,81]
Valuation of greenhouse gas emissions	189	378	568	GBP/tCO_2e	[80]

* n.a.: not available.

References

1. Sapsford, D.J.; Stewart, D.I.; Sinnett, D.E.; Burke, I.T.; Cleall, P.J.; Harbottle, M.J.; Mayes, W.; Owen, N.E.; Sardo, A.M.; Weightman, A. Circular economy landfills for temporary storage and treatment of mineral-rich wastes. *Proc. Inst. Civ. Eng. Waste Resour. Manag.* **2023**, *176*, 77–93. [CrossRef]
2. Wastling, T.; Charnley, F.; Moreno, M. Design for Circular Behaviour: Considering Users in a Circular Economy. *Sustainability* **2018**, *10*, 1743. [CrossRef]
3. Bjørnbet, M.M.; Skaar, C.; Fet, A.M.; Schulte, K.Ø. Circular economy in manufacturing companies: A review of case study literature. *J. Clean. Prod.* **2021**, *294*, 126268. [CrossRef]
4. Kirchherr, J.; Reike, D.; Hekkert, M. Conceptualizing the circular economy: An analysis of 114 definitions. *Resour. Conserv. Recycl.* **2017**, *127*, 221–232. [CrossRef]
5. Lambiase, N.; Barbera, F. The Anatomy of the Circular Economy: Goals, Strategies, Values and Scales. In *Innovations for Circularity and Knowledge Creation: Participation and Cooperative Approaches for Sustainability*; Bernardi, A., Mazzanti, M., Monni, S., Eds.; Springer Nature: Cham, Switzerland, 2024; pp. 21–41. [CrossRef]
6. Kisser, J.; Wirth, M.; De Gusseme, B.; Van Eekert, M.; Zeeman, G.; Schoenborn, A.; Vinnerås, B.; Finger, D.C.; Repinc, S.K.; Bulc, T.G.; et al. A review of nature-based solutions for resource recovery in cities. *Blue-Green Syst.* **2020**, *2*, 138–172. [CrossRef]
7. Mohammad, A.; Sapsford, D.; Harbottle, M.; Cleall, P.; Stewart, D.I.; Sepúlveda, F. Effect of Different Physical and Geochemical Parameters on Mobilisation of Metals: A Crucial Step Towards Resource Recovery from Waste. In Proceedings of the 9th International Congress on Environmental Geotechnics, Chania, Greece, 25–28 June 2022. [CrossRef]
8. Shaw, R.A.; Petavratzi, E.; Bloodworth, A.J. Resource Recovery from Mine Waste. In *Waste as a Resource*; Hester, R.E., Harrison, R.M., Harrison, R., Hester, R., Eds.; The Royal Society of Chemistry: London, UK, 2013; pp. 44–65. [CrossRef]
9. Sapsford, D.; Cleall, P.; Harbottle, M. In Situ Resource Recovery from Waste Repositories: Exploring the Potential for Mobilization and Capture of Metals from Anthropogenic Ores. *J. Sustain. Met.* **2017**, *3*, 375–392. [CrossRef]
10. Krook, J.; Svensson, N.; Eklund, M. Landfill mining: A critical review of two decades of research. *Waste Manag.* **2012**, *32*, 513–520. [CrossRef]
11. Dermatas, D. Waste management and research and the sustainable development goals: Focus on soil and groundwater pollution. *Waste Manag. Res.* **2017**, *35*, 453–455. [CrossRef]
12. Sinnett, D. Going to waste? The potential impacts on nature conservation and cultural heritage from resource recovery on former mineral extraction sites in England and Wales. *J. Environ. Plan. Manag.* **2019**, *62*, 1227–1248. [CrossRef]
13. Wuana, R.A.; Okieimen, F.E. Heavy Metals in Contaminated Soils: A Review of Sources, Chemistry, Risks and Best Available Strategies for Remediation. *ISRN Ecol.* **2011**, *2011*, 402647. [CrossRef]
14. Osra, F.A.; Elbisy, M.S.; Mosaıbah, H.A.; Osra, K.; Ciner, M.N.; Ozcan, H.K. Environmental Impact Assessment of a Dumping Site: A Case Study of Kakia Dumping Site. *Sustainability* **2024**, *16*, 3882. [CrossRef]
15. Yin, C.; Zhao, W.; Pereira, P. Soil conservation service underpins sustainable development goals. *Glob. Ecol. Conserv.* **2022**, *33*, e01974. [CrossRef]
16. Mead, I.; Apted, J.; Sharif, S. Delivering London 2012: Contaminated soil treatment at the Olympic Park. *Proc. Inst. Civ. Eng. Geotech. Eng.* **2013**, *166*, 8–17. [CrossRef]
17. Apted, M.J.; Ahn, J. (Eds.) *Geological Repository Systems for Safe Disposal of Spent Nuclear Fuels and Radioactive Waste*, 2nd ed.; Woodhead Publishing: Sawston, UK, 2017.
18. Alshehri, K.; Harbottle, M.; Sapsford, D.; Beames, A.; Cleall, P. Integration of ecosystem services and life cycle assessment allows improved accounting of sustainability benefits of nature-based solutions for brownfield redevelopment. *J. Clean. Prod.* **2023**, *413*, 137352. [CrossRef]
19. Alshehri, K.; Gao, Z.; Harbottle, M.; Sapsford, D.; Cleall, P. Life cycle assessment and cost-benefit analysis of nature-based solutions for contaminated land remediation: A mini-review. *Heliyon* **2023**, *9*, e20632. [CrossRef]
20. Ahmed, R.O.; Al-Mohannadi, D.M.; Linke, P. Multi-objective resource integration for sustainable industrial clusters. *J. Clean. Prod.* **2021**, *316*, 128237. [CrossRef]
21. Huntington, V.E.; Coulon, F.; Wagland, S.T. Innovative Resource Recovery from Industrial Sites: A Critical Review. *Sustainability* **2022**, *15*, 489. [CrossRef]
22. Fortunati, S.; Morea, D.; Mosconi, E.M. Circular economy and corporate social responsibility in the agricultural system: Cases study of the Italian agri-food industry. *Agric. Econ.* **2020**, *66*, 489–498. [CrossRef]
23. Alamerew, Y.A.; Kambanou, M.L.; Sakao, T.; Brissaud, D. A Multi-Criteria Evaluation Method of Product-Level Circularity Strategies. *Sustainability* **2020**, *12*, 5129. [CrossRef]
24. Basirati, M.; Jokar, M.R.A.; Hassannayebi, E. Bi-objective optimization approaches to many-to-many hub location routing with distance balancing and hard time window. *Neural Comput. Appl.* **2020**, *32*, 13267–13288. [CrossRef]
25. Baratsas, S.G.; Pistikopoulos, E.N.; Avraamidou, S. A systems engineering framework for the optimization of food supply chains under circular economy considerations. *Sci. Total. Environ.* **2021**, *794*, 148726. [CrossRef] [PubMed]
26. Holzkämper, A.; Klein, T.; Seppelt, R.; Fuhrer, J. Assessing the propagation of uncertainties in multi-objective optimization for agro-ecosystem adaptation to climate change. *Environ. Model. Softw.* **2015**, *66*, 27–35. [CrossRef]

27. Zolghadr-Asli, B.; Bozorg-Haddad, O.; Enayati, M.; Goharian, E. Developing a Robust Multi-Attribute Decision-Making Framework to Evaluate Performance of Water System Design and Planning under Climate Change. *Water Resour. Manag.* **2021**, *35*, 279–298. [CrossRef]
28. Beh, E.H.; Zheng, F.; Dandy, G.C.; Maier, H.R.; Kapelan, Z. Robust optimization of water infrastructure planning under deep uncertainty using metamodels. *Environ. Model. Softw.* **2017**, *93*, 92–105. [CrossRef]
29. Alshehri, K.; Harbottle, M.; Sapsford, D.; Cleall, P. Nature-based secondary resource recovery decision-making from regional and national lens: A mini-review. *Front. Sustain.* **2024**. *under review*.
30. Bayer, P.; Duran, E.; Baumann, R.; Finkel, M. Optimized groundwater drawdown in a subsiding urban mining area. *J. Hydrol.* **2009**, *365*, 95–104. [CrossRef]
31. Morano, P.; Tajani, F. The Transfer of Development Rights for the Regeneration of Brownfield Sites. *Appl. Mech. Mater.* **2013**, *409–410*, 971–978. [CrossRef]
32. De Mare, G.; Nesticò, A.; Tajani, F. The Rational Quantification of Social Housing. In *Computational Science and Its Applications—ICCSA 2012*; Murgante, B., Gervasi, O., Misra, S., Nedjah, A., Rocha, M.A.C., Taniar, D., Apduhan, B.O., Eds.; Lecture Notes in Computer Science; Springer: Berlin/Heidelberg, Germany, 2012; Volume 7334, pp. 27–43. [CrossRef]
33. Jeyasingh, J.; Somasundaram, V.; Philip, L.; Bhallamudi, S.M. Bioremediation of Cr(VI) contaminated soil/sludge: Experimental studies and development of a management model. *Chem. Eng. J.* **2010**, *160*, 556–564. [CrossRef]
34. Guo, M. Multi-scale system modelling under circular bioeconomy. *Comput. Aided Chem. Eng.* **2018**, *43*, 833–838. [CrossRef]
35. Robles, I.; Guo, M. Development of Systems Modelling Framework for Waste-to-Resource Transformation. *Comput. Aided Chem. Eng.* **2020**, *48*, 1597–1602. [CrossRef]
36. Robles, I.; Durkin, A.; Guo, M. Stochastic optimisation of organic waste-to-resource value chain. *Environ. Pollut.* **2021**, *273*, 116435. [CrossRef]
37. Huang, Y.; Xu, J. Bi-level multi-objective programming approach for bioenergy production optimization towards co-digestion of kitchen waste and rice straw. *Fuel* **2022**, *316*, 123117. [CrossRef]
38. Capraz, O.; Polat, O.; Gungor, A. Planning of waste electrical and electronic equipment (WEEE) recycling facilities: MILP modelling and case study investigation. *Flex. Serv. Manuf. J.* **2015**, *27*, 479–508. [CrossRef]
39. Wu, H.; Wan, Z. A multiobjective optimization model and an orthogonal design–based hybrid heuristic algorithm for regional urban mining management problems. *J. Air Waste Manag. Assoc.* **2018**, *68*, 146–169. [CrossRef]
40. Hernández, I.F.; Ordóñez, J.I.; Robles, P.A.; Gálvez, E.D.; Cisternas, L.A. A Methodology for Design and Operation Of Heap Leaching Systems. *Miner. Process. Extr. Met. Rev.* **2017**, *38*, 180–192. [CrossRef]
41. O'Dwyer, E.; Chen, K.; Wang, H.; Wang, A.; Shah, N.; Guo, M. Optimisation of wastewater treatment strategies in eco-industrial parks: Technology, location and transport. *Chem. Eng. J.* **2020**, *381*, 122643. [CrossRef]
42. Misrol, M.A.; Alwi, S.R.W.; Lim, J.S.; Manan, Z.A. Optimization of energy-water-waste nexus at district level: A techno-economic approach. *Renew. Sustain. Energy Rev.* **2021**, *152*, 111637. [CrossRef]
43. Singh, A.; Sarma, A.K.; Hack, J. Cost-Effective Optimization of Nature-Based Solutions for Reducing Urban Floods Considering Limited Space Availability. *Environ. Process.* **2020**, *7*, 297–319. [CrossRef]
44. Alves, A.; Vojinovic, Z.; Kapelan, Z.; Sanchez, A.; Gersonius, B. Exploring trade-offs among the multiple benefits of green-blue-grey infrastructure for urban flood mitigation. *Sci. Total. Environ.* **2020**, *703*, 134980. [CrossRef]
45. McClymont, K.; Cunha, D.G.F.; Maidment, C.; Ashagre, B.; Vasconcelos, A.F.; de Macedo, M.B.; dos Santos, M.F.N.; Júnior, M.N.G.; Mendiondo, E.M.; Barbassa, A.P.; et al. Towards urban resilience through Sustainable Drainage Systems: A multi-objective optimisation problem. *J. Environ. Manag.* **2020**, *275*, 111173. [CrossRef] [PubMed]
46. Liu, L.; Dobson, B.; Mijic, A. Optimisation of urban-rural nature-based solutions for integrated catchment water management. *J. Environ. Manag.* **2023**, *329*, 117045. [CrossRef] [PubMed]
47. Liu, Y.; Xia, C.; Ou, X.; Lv, Y.; Ai, X.; Pan, R.; Zhang, Y.; Shi, M.; Zheng, X. Quantitative structure and spatial pattern optimization of urban green space from the perspective of carbon balance: A case study in Beijing, China. *Ecol. Indic.* **2023**, *148*, 110034. [CrossRef]
48. Castro, C. Optimizing nature-based solutions by combining social equity, hydro-environmental performance, and economic costs through a novel Gini coefficient. *J. Hydrol. X* **2022**, *16*, 100127. [CrossRef]
49. Yang, S.; Ruangpan, L.; Torres, A.S.; Vojinovic, Z. Multi-objective Optimisation Framework for Assessment of Trade-Offs between Benefits and Co-benefits of Nature-based Solutions. *Water Resour. Manag.* **2023**, *37*, 2325–2345. [CrossRef]
50. Yang, G.; Best, E.P. Spatial optimization of watershed management practices for nitrogen load reduction using a modeling-optimization framework. *J. Environ. Manag.* **2015**, *161*, 252–260. [CrossRef] [PubMed]
51. Feng, S.; Shen, J.; Sheng, S.; Hu, Z.; Wang, Y. Spatial Prioritizing Brownfields Catering for Green Infrastructure by Integrating Urban Demands and Site Attributes in a Metropolitan Area. *Land* **2023**, *12*, 802. [CrossRef]
52. Bhakuni, P.; Das, A. An Innovative Algorithm-Driven Optimization Framework for Landfill Mining: Aiming Sustainable Profitability Expeditiously. *IEEE Access* **2023**, *11*, 122792–122820. [CrossRef]
53. Hutahaean, J.; Demyanov, V.; Christie, M. Reservoir development optimization under uncertainty for infill well placement in brownfield redevelopment. *J. Pet. Sci. Eng.* **2019**, *175*, 444–464. [CrossRef]
54. Seddon, N.; Smith, A.; Smith, P.; Key, I.; Chausson, A.; Girardin, C.; House, J.; Srivastava, S.; Turner, B. Getting the message right on nature-based solutions to climate change. *Glob. Chang. Biol.* **2021**, *27*, 1518–1546. [CrossRef]

55. García, J.; Peña, A. Robust Optimization: Concepts and Applications. In *Nature-Inspired Methods for Stochastic, Robust and Dynamic Optimization*; Del Ser, J., Osaba, E., Eds.; IntechOpen: London, UK, 2018. [CrossRef]
56. Meysami, R.; Niksokhan, M.H. Evaluating robustness of waste load allocation under climate change using multi-objective decision making. *J. Hydrol.* **2020**, *588*, 125091. [CrossRef]
57. Wang, M.; Yu, H.; Jing, R.; Liu, H.; Chen, P.; Li, C. Combined multi-objective optimization and robustness analysis framework for building integrated energy system under uncertainty. *Energy Convers. Manag.* **2020**, *208*, 112589. [CrossRef]
58. Alshehri, K.; Chen, I.-C.; Rugani, B.; Sapsford, D.; Harbottle, M.; Cleall, P. A novel uncertainty assessment protocol for integrated ecosystem services-life cycle assessments: A comparative case of nature-based solutions. *Sustain. Prod. Consum.* **2024**, *47*, 499–515. [CrossRef]
59. Mišković, S.; Stanimirović, Z.; Grujičić, I. Solving the robust two-stage capacitated facility location problem with uncertain transportation costs. *Optim. Lett.* **2017**, *11*, 1169–1184. [CrossRef]
60. Sayers, P.; Penning-Rowsell, E.C.; Horritt, M. Flood vulnerability, risk, and social disadvantage: Current and future patterns in the UK. *Reg. Environ. Chang.* **2018**, *18*, 339–352. [CrossRef]
61. Mavrotas, G. Effective implementation of the ε-constraint method in Multi-Objective Mathematical Programming problems. *Appl. Math. Comput.* **2009**, *213*, 455–465. [CrossRef]
62. Basirati, M.; Billot, R.; Meyer, P.; Bocher, E. Exact Zoning Optimization Model for Marine Spatial Planning (MSP). *Front. Mar. Sci.* **2021**, *8*, 726187. [CrossRef]
63. Mavrotas, G.; Florios, K. An improved version of the augmented ε-constraint method (AUGMECON2) for finding the exact pareto set in multi-objective integer programming problems. *Appl. Math. Comput.* **2013**, *219*, 9652–9669. [CrossRef]
64. Riley, A. Slag Composition Data for: Legacy Iron and Steel Wastes in the UK: Extent, Resource Potential, and Management Futures. Available online: https://data.mendeley.com/datasets/dzxx4wh75n/1 (accessed on 10 October 2023).
65. Carey, M.A. *Guidance on the Assessment and Monitoring of Natural Attentuation of Contaminants in Groundwater*; Environment Agency: Bristol, UK, 2000.
66. Johnson, D.B. Biomining—Biotechnologies for extracting and recovering metals from ores and waste materials. *Curr. Opin. Biotechnol.* **2014**, *30*, 24–31. [CrossRef]
67. Johnson, D.B. The Evolution, Current Status, and Future Prospects of Using Biotechnologies in the Mineral Extraction and Metal Recovery Sectors. *Minerals* **2018**, *8*, 343. [CrossRef]
68. Lusty, P.; Shaw, R.; Gunn, A.; Idoine, N. *UK Criticality Assessment of Technology Critical Minerals and Metals*; British Geological Survey: Nottingham, UK, 2021.
69. European Commission. Directorate General for Internal Market, Industry, Entrepreneurship and SMEs. Study on the Critical Raw Materials for the EU 2023: Final Report. LU: Publications Office. 2023. Available online: https://data.europa.eu/doi/10.2873/725585 (accessed on 27 May 2024).
70. Sigman, H. Environmental Liability and Redevelopment of Old Industrial Land. *J. Law Econ.* **2010**, *53*, 289–306. [CrossRef]
71. UK Government. Brownfield Land Dataset | Planning Data. Available online: https://www.planning.data.gov.uk/dataset/brownfield-land (accessed on 21 May 2024).
72. Schedules of Contractors Equipment, Rates for Use on Construction Contracts, Civil Engineering Contractors Association, London, 978-1-9161584-2-9. 2019. Available online: http://www.ceca.co.uk/ (accessed on 15 September 2023).
73. Greenhouse Gas Reporting: Conversion Factors 2023. Available online: https://www.gov.uk/government/publications/greenhouse-gas-reporting-conversion-factors-2023 (accessed on 15 August 2023).
74. Riley, A.L.; MacDonald, J.M.; Burke, I.T.; Renforth, P.; Jarvis, A.P.; Hudson-Edwards, K.A.; McKie, J.; Mayes, W.M. Legacy iron and steel wastes in the UK: Extent, resource potential, and management futures. *J. Geochem. Explor.* **2020**, *219*, 106630. [CrossRef]
75. Raes, L.; Mittempergher, D.; Piaggio, M.; Siikamäki, J. *Nature-Based Recovery Can Create Jobs, Deliver Growth and Provide Value for Nature*; IUCN: Gland, Switzerland, 2021.
76. Jorat, M.E.; Goddard, M.A.; Manning, P.; Lau, H.K.; Ngeow, S.; Sohi, S.P.; Manning, D.A. Passive CO2 removal in urban soils: Evidence from brownfield sites. *Sci. Total. Environ.* **2020**, *703*, 135573. [CrossRef]
77. UK Critical Minerals Intelligence Centre. CMIC Web GIS Live. CMIC INTERACTIVE MAP. Available online: https://experience.arcgis.com/experience/6306721821554bbd8447802676695588 (accessed on 21 May 2024).
78. The London Metal Exchange. LME Cobalt. Available online: https://www.lme.com/Metals/EV/LME-Cobalt (accessed on 12 January 2024).
79. SMM Metal Market. Refined Cobalt Price Today | Historical Refined Cobalt Price Charts. Available online: https://www.metal.com/Cobalt/201102250375 (accessed on 12 January 2024).
80. The London Metal Exchange. LME Nickel. Available online: https://www.lme.com/Metals/Non-ferrous/LME-Nickel (accessed on 12 January 2024).
81. SMM Metal Market. Nickel Price Today | Historical Base Metals Price Charts. Available online: https://www.metal.com/price/Base%20Metals/Nickel (accessed on 12 January 2024).
82. Boundary-LineTM [SHAPE Geospatial Data], Scale 1:10000', Tiles: GB. Ordnance Survey (GB), Mar. 28, 2023. Available online: https://digimap.edina.ac.uk (accessed on 23 August 2023).

83. OS Open Roads [SHAPE Geospatial Data], Scale 1:25000′, Tiles: Hp, ht, hu, hy, hz, na, nb, nc, nd, nf, ng, nh, nj, nk, nl, nm, nn, no, nr, ns, nt, nu, nw, nx, ny, nz, sd, se, sh, sj, sk, sm, sn, so, sp, sr, ss, st, su, sv, sw, sx, sy, sz, ta, tf, tg, tl, tm, tq, tr, tv. Ordnance Survey (GB), Apr. 21, 2023. Available online: https://digimap.edina.ac.uk (accessed on 21 August 2023).
84. Valuation of Greenhouse Gas Emissions: For Policy Appraisal and Evaluation. Available online: https://www.gov.uk/government/publications/valuing-greenhouse-gas-emissions-in-policy-appraisal/valuation-of-greenhouse-gas-emissions-for-policy-appraisal-and-evaluation (accessed on 1 November 2023).
85. Nikas, A.; Fountoulakis, A.; Forouli, A.; Doukas, H. A robust augmented ε-constraint method (AUGMECON-R) for finding exact solutions of multi-objective linear programming problems. *Oper. Res.* **2022**, *22*, 1291–1332. [CrossRef]
86. Zitzler, E.; Thiele, L.; Laumanns, M.; Fonseca, C.; da Fonseca, V. Performance assessment of multiobjective optimizers: An analysis and review. *IEEE Trans. Evol. Comput.* **2003**, *7*, 117–132. [CrossRef]
87. Basirati, M.; Billot, R.; Meyer, P. An Extension of NSGA-II for Scaling up Multi-objective Spatial Zoning Optimization. In *Learning and Intelligent Optimization*; Simos, D.E., Rasskazova, V.A., Archetti, F., Kotsireas, I.S., Pardalos, P.M., Eds.; Lecture Notes in Computer Science; Springer: Cham, Switzerland, 2022; Volume 13621, pp. 205–219. [CrossRef]
88. Pătrăușanu, A.; Florea, A.; Neghină, M.; Dicoiu, A.; Chiș, R. A Systematic Review of Multi-Objective Evolutionary Algorithms Optimization Frameworks. *Processes* **2024**, *12*, 869. [CrossRef]
89. Basirati, M.; Billot, R.; Meyer, P. Two parameter-tuned multi-objective evolutionary-based algorithms for zoning management in marine spatial planning. *Ann. Math. Artif. Intell.* **2023**, 1–32. [CrossRef]
90. Ishibuchi, H.; Imada, R.; Setoguchi, Y.; Nojima, Y. How to Specify a Reference Point in Hypervolume Calculation for Fair Performance Comparison. *Evol. Comput.* **2018**, *26*, 411–440. [CrossRef]
91. Udías, A.; Efremov, R.; Cano, J. *Methodological Review of Multicriteria Optimization Techniques: Aplications in Water Resources*; Technical Report 2012.1; Centro de Servicios en Gestión de Información (CESGI): Buenos Aires, Argentina, 2012.
92. Opricovic, S.; Tzeng, G.-H. Compromise solution by MCDM methods: A comparative analysis of VIKOR and TOPSIS. *Eur. J. Oper. Res.* **2004**, *156*, 445–455. [CrossRef]
93. Štilić, A.; Puška, A. Integrating Multi-Criteria Decision-Making Methods with Sustainable Engineering: A Comprehensive Review of Current Practices. *Eng* **2023**, *4*, 1536–1549. [CrossRef]
94. Hwang, C.-L.; Yoon, K. *Multiple Attribute Decision Making: Methods and Applications a State-of-the-Art Survey*; Springer Science & Business Media: Berlin, Germany, 2012; Volume 186.
95. Brans, J.-P.; Vincke, P. A Preference Ranking Organisation Method: (The PROMETHEE Method for Multiple Criteria Decision-Making). *Manag. Sci.* **1985**, *31*, 647–656. [CrossRef]
96. Monardes, V.; Sepúlveda, J.M. Multi-Criteria Analysis for Circular Economy Promotion in the Management of Tailings Dams: A Case Study. *Minerals* **2023**, *13*, 486. [CrossRef]
97. Wismans, L.J.; Brands, T.; Van Berkum, E.C.; Bliemer, M.C. Pruning and ranking the Pareto optimal set, application for the dynamic multi-objective network design problem. *J. Adv. Transp.* **2014**, *48*, 588–607. [CrossRef]
98. Spearman, C. The Proof and Measurement of Association between Two Things. *Am. J. Psychol.* **1904**, *15*, 72–101. [CrossRef]
99. Kendall, M.G. A New Measure of Rank Correlation. *Biometrika* **1938**, *30*, 81. [CrossRef]
100. Mitchell, S.; OSullivan, M.; Dunning, I. *Pulp: A linear Programming Toolkit for Python*; The University of Auckland: Auckland, New Zealand, 2011; Volume 65.
101. Raffler, C. QNEAT3—QGIS Network Analysis Toolbox 3. GitHub. 2023. Available online: https://github.com/root676/QNEAT3 (accessed on 21 May 2024).
102. IBM. ILOG CPLEX Optimization Studio V22.1: User's Manual. 2019. Available online: https://www.ibm.com/docs/en/icos/12.9.0 (accessed on 21 May 2024).
103. Virtanen, P.; Gommers, R.; Oliphant, T.E.; Haberland, M.; Reddy, T.; Cournapeau, D.; Burovski, E.; Peterson, P.; Weckesser, W.; Bright, J.; et al. SciPy 1.0 Contributors. SciPy 1.0 Fundamental Algorithms for Scientific Computing in Python. *Nat. Methods* **2020**, *17*, 261–272. [CrossRef]
104. Kizielewicz, B.; Shekhovtsov, A.; Sałabun, W. pymcdm—The universal library for solving multi-criteria decision-making problems. *SoftwareX* **2023**, *22*, 101368. [CrossRef]
105. Demir, I.; Ergin, F.C.; Kiraz, B. A New Model for the Multi-Objective Multiple Allocation Hub Network Design and Routing Problem. *IEEE Access* **2019**, *7*, 90678–90689. [CrossRef]
106. Maadanpour Safari, F.; Etebari, F.; Pourghader Chobar, A. Modelling and optimization of a tri-objective Transportation-Location-Routing Problem considering route reliability: Using MOGWO, MOPSO, MOWCA and NSGA-II. *J. Optim. Ind. Eng.* **2021**, *14*, 83–98. [CrossRef]
107. Li, P.; Qian, H.; Wu, J.; Chen, J. Sensitivity analysis of TOPSIS method in water quality assessment: I. Sensitivity to the parameter weights. *Environ. Monit. Assess.* **2013**, *185*, 2453–2461. [CrossRef]
108. Genc, T. Sensitivity analysis on PROMETHEE and TOPSIS weights. *Int. J. Manag. Decis. Mak.* **2014**, *13*, 403. [CrossRef]
109. Venkat, V.; Jacobson, S.H.; Stori, J.A. A Post-Optimality Analysis Algorithm for Multi-Objective Optimization. *Comput. Optim. Appl.* **2004**, *28*, 357–372. [CrossRef]
110. Deb, K.; Jain, H. An Evolutionary Many-Objective Optimization Algorithm Using Reference-Point-Based Nondominated Sorting Approach, Part I: Solving Problems with Box Constraints. *IEEE Trans. Evol. Comput.* **2014**, *18*, 577–601. [CrossRef]

111. Basirati, M. Zoning Management in Marine Spatial Planning: Multi-Objective Optimization and Agent-Based Conflict Resolution. Ph.D. Thesis, IMT Atlantique, Nantes, France, 2022.
112. Raidl, G.R.; Puchinger, J.; Blum, C. Handbook of Metaheuristics. In *International Series in Operations Research & Management Science*; Springer: Cham, Switzerland, 2019; Volume 272.
113. Kwatra, S.; Kumar, A.; Sharma, S.; Sharma, P. Stakeholder participation in prioritizing sustainability issues at regional level using analytic hierarchy process (AHP) technique: A case study of Goa, India. *Environ. Sustain. Indic.* **2021**, *11*, 100116. [CrossRef]
114. Kibria, A.S.; Seekamp, E.; Xiao, X.; Dalyander, S.; Eaton, M. Multi-criteria decision approach for climate adaptation of cultural resources along the Atlantic coast of the southeastern United States: Application of AHP method. *Clim. Risk Manag.* **2024**, *43*, 100587. [CrossRef]
115. Iacovidou, E.; Velis, C.A.; Purnell, P.; Zwirner, O.; Brown, A.; Hahladakis, J.; Millward-Hopkins, J.; Williams, P.T. Metrics for optimising the multi-dimensional value of resources recovered from waste in a circular economy: A critical review. *J. Clean. Prod.* **2017**, *166*, 910–938. [CrossRef]
116. Greco, S.; Ishizaka, A.; Tasiou, M.; Torrisi, G. On the Methodological Framework of Composite Indices: A Review of the Issues of Weighting, Aggregation, and Robustness. *Soc. Indic. Res.* **2019**, *141*, 61–94. [CrossRef]
117. Kahraman, C.; Ruan, D.; Dogan, I. Fuzzy group decision-making for facility location selection. *Inf. Sci.* **2003**, *157*, 135–153. [CrossRef]
118. Anjum, M.; Min, H.; Ahmed, Z. Healthcare Waste Management through Multi-Stage Decision-Making for Sustainability Enhancement. *Sustainability* **2024**, *16*, 4872. [CrossRef]
119. Yousefpour, R.; Temperli, C.; Jacobsen, J.B.; Thorsen, B.J.; Meilby, H.; Lexer, M.J.; Lindner, M.; Bugmann, H.; Borges, J.G.; Palma, J.H.N.; et al. A framework for modeling adaptive forest management and decision making under climate change. *Ecol. Soc.* **2017**, *22*, art40. [CrossRef]
120. Bertsimas, D.; Goyal, V. On the Power of Robust Solutions in Two-Stage Stochastic and Adaptive Optimization Problems. *Math. Oper. Res.* **2010**, *35*, 284–305. [CrossRef]